Progress in Oceanography 96 (2012) 14–39

Contents lists available at SciVerse ScienceDirect

Progress in Oceanography

journal homepage: www.elsevier.com/locate/pocean

Mesoscale eddies in the Gulf of Aden and their impact on the spreading of Red Sea Outflow Water

Amy S. Bower *, Heather H. Furey

Department of Physical Oceanography, Woods Hole Oceanographic Institution, Woods Hole, MA 02543, USA

ARTICLE INFO

Article history:
Received 29 November 2010
Received in revised form 6 September 2011
Accepted 18 September 2011
Available online 10 October 2011

ABSTRACT

The Gulf of Aden (GOA) in the northwestern Indian Ocean is the receiving basin for Red Sea Outflow Water (RSOW), one of the World's few high-salinity dense overflows, but relatively little is known about spreading pathways and transformation of RSOW through the gulf. Here we combine historical data, satellite altimetry, new synoptic hydrographic surveys and the first *in situ* direct observations of subsurface currents in the GOA to identify the most important processes in the spreading of RSOW. The new *in situ* data sets were collected in 2001–2003 as part of the Red Sea Outflow Experiment (REDSOX) and consist of two CTD/LADCP Surveys and 49 one-year trajectories from acoustically tracked floats released at the depth of RSOW.

The results indicate that the prominent positive and negative sea level anomalies frequently observed in the GOA with satellite altimetry are associated with anticyclonic and cyclonic eddies that often reach to at least 1000 m depth, i.e., through the depth range of equilibrated RSOW. The eddies dominate RSOW spreading pathways and help to rapidly mix the outflow water with the background. Eddies in the central and eastern gulf are basin-scale (~250-km diameter) and have maximum azimuthal speeds of about 30 cm/s at the RSOW level. In the western gulf, smaller eddies not detectable with satellite altimetry appear to form as the larger westward-propagating eddies impale themselves on the high ridges flanking the Tadjura Rift. Both the hydrographic and Lagrangian observations show that eddies originating outside the gulf often transport a core of much cooler, fresher water from the Arabian Sea all the way to the western end of the GOA, where the highest-salinity outflow water is found. This generates large vertical and horizontal gradients of temperature and salinity, setting up favorable conditions for salt fingering and diffusive convection. Both of these mixing processes were observed to be active in the gulf.

Two new annually appearing anticyclonic eddies are added to the previously identified Gulf of Aden Eddy (GAE; Prasad and Ikeda, 2001) and Somali Current Ring (SCR; Fratantoni et al., 2006). These are the Summer Eddy (SE) and the Lee Eddy (LE), both of which form at the beginning of the summer monsoon when strong southwest winds blowing through Socotra Passage effectively split the GAE into two smaller eddies. The SE strengthens as it propagates westward deeper in the GOA, while the Lee Eddy remains stationary in the lee of Socotra Island. Both eddies are strengthened or sustained by Ekman convergence associated with negative wind stress curl patches caused by wind jets through or around high orography. The annual cycle in the appearance, propagation and demise of these new eddies and those described in earlier work is documented to provide a comprehensive view of the most energetic circulation features in the GOA.

The observations contain little evidence of features that have been shown previously to be important in the spreading of Mediterranean Outflow Water (MOW) in the North Atlantic, namely a wall-bounded subsurface jet (the Mediterranean Undercurrent) and submesoscale coherent lenses containing a core of MOW ('meddies'). This is attributed to the fact that the RSOW enters the open ocean on a western boundary. High background eddy kinetic energy typical of western boundary regimes will tend to shear apart submesoscale eddies and boundary undercurrents. Even if a submesoscale lens of RSOW did form in the GOA, westward self-propagation would transport the eddy and its cargo of outflow water back toward, rather than away from, its source.

1. Introduction

The Gulf of Aden (GOA) is a large, deep rectangular basin that connects the Red Sea to the Arabian Sea in the northwestern Indian Ocean, Fig. 1. Even though the GOA is the receiving basin for one of

* Corresponding author.
E-mail address: abower@whoi.edu (A.S. Bower).

0079-6611/$ - see front matter © 2011 Elsevier Ltd. All rights reserved.
doi:10.1016/j.pocean.2011.09.003

the World's few high-salinity dense overflows, namely Red Sea Water (salinity ~40 psu), the region has received little attention recently from oceanographers due to political instability in nearby countries and threats of piracy. We know from historical studies that the salty Red Sea Water flows over the 160-m deep sill in Bab al Mandeb Strait and entrains cooler, fresher Gulf of Aden Intermediate Water (GAIW) as it descends to intermediate depths in the western GOA (Siedler, 1968; Wyrtki, 1971; Fedorov and Meshchanov, 1988; Murray and Johns, 1997). Large-scale hydrographic observations in the Indian Ocean show that the resultant gravitationally equilibrated Red Sea Outflow Water (RSOW) leaves the GOA and enters the Arabian Sea with a much lower salinity (~35.7; Beal et al., 2000) that nonetheless can be traced throughout much of the Indian Ocean as a mid-depth salinity maximum (e.g., Beal et al., 2000). It is also known that unlike the Mediterranean outflow, the Red Sea outflow undergoes large seasonal modulation in transport through Bab al Mandeb, with the maximum occurring during the winter monsoon (~0.6–0.7 Sv) and a near-zero minimum during summer (Murray and Johns, 1997). But the pathways by which RSOW spreads through the GOA and the processes that transform its water properties along those pathways are not well-known.

In 2001, the first comprehensive *in situ* study of GOA circulation and hydrography was conducted as part of the Red Sea Outflow Experiment (REDSOX), a collaborative effort by the Woods Hole Oceanographic Institution and the Rosenstiel School of Marine and Atmospheric Science. It included two quasi-synoptic hydrographic surveys of the GOA at the peaks of the winter and summer monsoon seasons and the release of 53 acoustically tracked floats at the depth of RSOW. The goals of this project were twofold. First, we sought to improve our understanding of the modification of RSW as it descends as a gravity current into the GOA (Ozgokmen et al., 2003; Peters and Johns, 2005; Peters et al., 2005; Bower et al., 2005; Matt and Johns, 2007; Chang et al., 2008; Ilicak et al., 2008a,b; Ilicak et al., 2011). Second we wanted to make the first subsurface measurements of GOA circulation and determine its impact on the stirring and mixing of the equilibrated RSOW. Two studies focused on this second goal revealed the presence of strong deep-reaching mesoscale eddies in the GOA and their potential impact on the spreading of RSOW. Bower et al. (2002) showed using direct velocity and hydrographic observations that during the first REDSOX survey, three energetic (surface speeds up to 50 cm/s) cyclonic and anticyclonic eddies were present in the gulf. They found that the eddy currents in some cases extended to nearly the ~2000 m-deep sea floor and appeared to strongly impact the spreading pathways of the recently injected RSOW at intermediate depths (300–800 m). Fratantoni et al. (2006) showed with remote sensing and hydrographic observations that one of the observed anticyclonic eddies appears at the entrance to the gulf nearly every year at the end of the summer monsoon (November) and propagates westward into the gulf during the winter. They further showed that this anticyclone results from a northward transport anomaly through Socotra Passage of relatively warm, fresh Somali Current water. The process was likened to the formation of North Brazil Current Rings from a retroflection of the North Brazil Current, and the GOA version was dubbed the Somali Current Ring (SCR) by Fratantoni et al. (2006) in recognition of this similarity.

Two other studies have described mesoscale eddies in the GOA. Prasad and Ikeda (2001) used historical hydrographic and drifter data as well as altimetric observations to show that a large (~600 km wide) anticyclonic eddy, called the "Gulf of Aden Eddy" (GAE) appears at the entrance to the GOA every year at the end of the winter monsoon (May), centered at about 13°N, 53°E. Surface velocities were estimated to be 30–50 cm s^{-1}, and it was argued that eddy currents extend down to 250 m assuming a level of no motion at 400 m. Prasad and Ikeda (2001) also argued that at least in some years, the appearance of the GAE was associated with the arrival at the western boundary of the Southern Arabian Sea High (SAH), which propagates across the Arabian Sea between February and April in the latitude band 4–8°N. The subsequent demise of the GAE was not discussed in their paper.

Al Saafani et al. (2007) used 11 years of altimetric-derived sea level anomaly (SLA) observations (1993–2003) to investigate the origin of mesoscale eddies in the GOA. They argued that anticyclonic and cyclonic eddies observed in the GOA owe their existence to several different mechanisms: Rossby waves radiating from the west coast of India (see e.g., Brandt et al., 2002), Rossby waves gen-

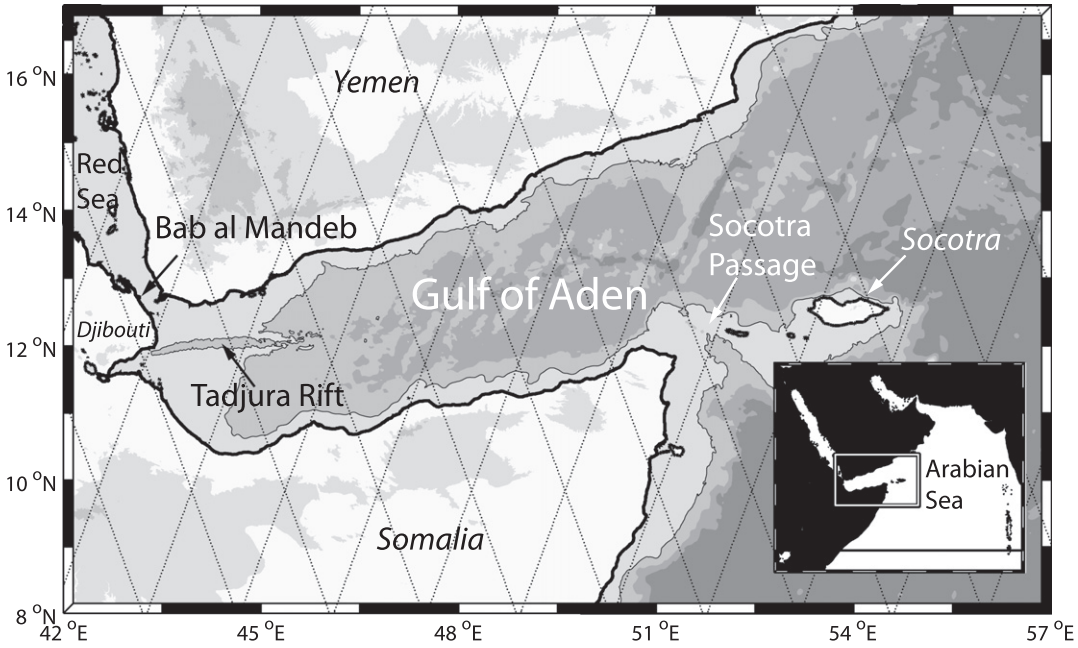

Fig. 1. Bathymetry, topography, and geographic locations in the Gulf of Aden and the northwestern Indian Ocean. Bathymetry and topography have been shaded every 1000 m. The thick solid bold black line designates the land-sea boundary, and the thinner black line delineates the 1000 m isobath. Topex/Poseidon and Jason-1 satellite tracks have been overlaid as dotted lines.

erated in the interior Arabian Sea, from instabilities of the Somali Current and its associated gyres (Great Whirl, Socotra Gyre) and to a lesser extent from local Ekman pumping. They showed that during winter, the eddies propagated westward at a speed predicted by the first baroclinic mode Rossby wave speed for the local stratification, 6.0–8.5 cm/s. They claimed that little or no westward propagation of eddies occurs in the GOA during the summer monsoon due to blocking by an area of low SLA at the gulf entrance.

Three studies have previously addressed the spreading pathways of RSOW in the GOA. Fedorov and Meshchanov (1988) used historical salinity data from the oceanographic archives of the former Soviet Union to describe RSOW pathways in the western gulf, but none of the original data were shown and the results were only illustrated schematically. Bower et al. (2000) used sparse historical salinity observations and four high-resolution AXBT surveys conducted by the US Naval Oceanographic Office (NAVOCEANO) in 1992–1993 to examine the distributions of RSOW in the GOA. They showed that the warmest (and presumably the most saline) outflow water was often found in the southwestern gulf and in various veins and blobs in the interior. Without salinity data to accompany the AXBT data and/or direct velocity observations, it was not possible in this study to determine the mechanisms leading to the spreading of RSOW and its transformation through the gulf. Finally, a recent modeling study (using a high resolution 3D regional model: Regional Ocean Modeling System; Ilicak et al., 2011) shows how the RSOW is transported from the Tadjura Rift out of the gulf to 48°E. They ran the model both with idealized circulation conditions (no eddies, a single cyclonic eddy, and a single anticyclonic eddy), and forced with 1 years' worth of 1/12° HYCOM data. Ilicak et al. (2011) show that the outflow, with no large scale eddies present, will form a boundary current along the southern boundary. When a single eddy is present, the boundary current is disrupted, with a cyclone enhancing transport of RSOW out of the GOA, and an anticyclone prohibiting this transport. Under more realistic external forcing conditions, the outflow is patchy, and occurs in bursts due to eddy circulation, with water from the Tadjura Rift taking less than 50 days to pass east of 48°N.

The purpose of this paper is to bring together the extensive direct velocity, hydrographic and Lagrangian data sets collected during both REDSOX surveys, most of which have not been previously published, with historical and remote sensing observations to provide a comprehensive description of the subsurface structure and evolution of mesoscale eddies in the GOA and their impact on RSOW spreading. The results show the GOA to be a region of strong mesoscale variability that effectively stirs and mixes RSOW with the background, producing a highly diluted new product that is ultimately discharged into the Arabian Sea. Double-diffusive mixing processes are also shown to be active in the GOA, mainly associated with recently injected overflow water. The Lagrangian data reveal the capacity of the eddies to trap fresher Indian Ocean water and transport it all the way to the western end of the gulf. We also show that much of the mesoscale variability is not random, but associated with a clear annual cycle in the appearance, propagation and decay of eddies, including but not limited to the GAE and SCR. The data sets used in this study are described in detail in Section 2. We begin Section 3 with a description of Gulf eddies observed in the AXBT surveys in the early 1990s and their signature in maps of SLA. We then go on to present hydrographic, direct velocity and Lagrangian observations from the 2001 REDSOX expeditions, including observations of double diffusive mixing. Again, maps of sea level anomaly are used to provide the large-scale spatial and temporal context for the *in situ* observations. Section 3 ends with an analysis of the annual cycle, its relationship to local wind forcing and a synthesis of new and historical observations of the eddies. The results are discussed and summarized in Section 4, which includes some thoughts on the different mechanisms by which RSOW and the better-known Mediterranean Outflow Water (MOW) spread away from their respective sources.

2. Data sources

2.1. Air-deployed expendable bathythermograph (AXBT) surveys

Between 1992 and 1995, NAVOCEANO conducted nine AXBT surveys in the GOA using 400-m and 800-m probes. Four of these were high-resolution gridded surveys with profile spacing of about 30 nm and consisting of more than 210 profiles, conducted in a quasi-seasonal sequence beginning in October 1992. [11–15 October 1992: 210 profiles; 1–7 March 1993: 220 profiles; 1–6 June 1993: 248 profiles; 21–31 August 1993: 216 profiles.] These data were used by Bower et al. (2000) to study the distribution of RSOW in the depth range 300–800 m based on temperature maps and the location of temperature inversions associated with equilibrated RSOW. The influence of the mesoscale eddy field on those distributions was not discussed in that earlier work. The accuracy of temperature and depth from the AXBTs is about ±0.2 °C and ±5 m (Boyd, 1986). In this paper we use only the upper 400 m of the profiles to map the thermocline depth and eddy structure throughout the gulf.

2.2. REDSOX hydrographic, direct-velocity, and float data

Two hydrographic and direct-velocity surveys of the Gulf of Aden were carried out in 2001 as part of REDSOX, the first in February–March 2001 on board the *R/V Knorr* (the "winter" cruise), and the second during August–September 2001 on board the *R/V Maurice Ewing* (the "summer" cruise). On both cruises, over 200 conductivity–temperature–depth (CTD)-lowered acoustic doppler profiler (LADCP) stations to 2000 m or the sea floor were occupied throughout Bab al Mandeb and the open gulf using a Sea-Bird Electronics, Inc. SBE911+ CTD system and a lowered 300 kHz broadband Teledyne RD Instruments, Inc. "Workhorse" ADCP. These data are described in detail in Johns et al. (2001) and Peters et al. (2005), respectively. LADCP accuracy is estimated to be ±3 cm s^{-1} (Peters and Johns, 2005). Some of the winter cruise data were previously presented by Bower et al. (2002). Here we will present a detailed analysis of both the summer and winter observations. The station locations for the two surveys were planned to be the same, but a pirate attack on the vessel during REDSOX-2 led to restrictions in vessel movement to outside 50 km from the coasts of Yemen and Somalia.

Also as part of REDSOX, a total of 53 isobaric RAFOS floats (Rossby et al., 1986) were released during the winter and summer cruises at 650 m and tracked for 1-year missions using an array of five 780-Hz acoustic sound sources (Furey et al., 2005). Nineteen of these were initially anchored to the seafloor at four "time series" sites and released their anchors at 2-month intervals. The remaining 34 floats were released from the *R/V Knorr* and *R/V Maurice Ewing* during the two cruises and began their drifting missions immediately. Position fixes were recorded four times daily, to accurately resolve eddy-scale motion, and temperature and pressure observations were recorded twice daily. The pressure and temperature were derived from a module manufactured and calibrated at Seascan, Inc., and accuracy is estimated to be ±5 dbars and ±0.005 °C, respectively. The sequential float releases meant that Lagrangian data were collected from February 2001 through March 2003. Nearly all the floats remained within the Gulf of Aden for their entire 1-year mission. A total of 41 float-years of data were collected. Some of these data (10 floats) have been used previously to describe pathways of Red Sea Outflow Water in the extreme western GOA/Tadjura Rift (Bower et al., 2005). Here, we use the full float data set to describe eddy characteristics and evolution in the entire GOA.

2.3. Altimetric observations

Sea surface height anomaly, or sea level anomaly (SLA), data were derived from quality controlled satellite altimetry data provided by AVISO (www.aviso.oceanobs.com). Ducet et al. (2000b) and Le Traon and Dibarboure (1999) detail the data processing used on and the accuracy of the altimetric measurements. The data were derived from a merged data set of all available satellites (TOPEX/Poseidon, Jason-1, ERS-1/2, and Envisat), available from 14 October 1992, to 5 January 2005. The altimeter product was gridded spatially at 1/3° × 1/3° on a Mercator grid and temporally at a 7-day interval, and detrended with a 7-year mean. The ground track spacing changed from a maximum of ~300 km in 1992 down to ~150 km by 2005. AVISO provides a historical summary of operational periods for each satellite mission at http://www.aviso.oceanobs.com/en/data/products/sea-surface-height-products/global/sla/index.html#c5134. We focused on the region 0–32°N and 42–70°E, the Gulf of Aden and Arabian Sea.

3. Results

3.1. Horizontal and vertical structure of mesoscale eddies in the GOA

3.1.1. 1992–1993: Repeated AXBT surveys

The set of four quasi-seasonal AXBT surveys conducted in the GOA by NAVOCEANO in 1992–1993 (Bower et al., 2000) is the only known high-resolution *in situ* data set in the GOA obtained prior to REDSOX. Before describing the structure of GOA eddies in these surveys, a 1-year time series of AVISO SLA in the GOA is used to set the temporal context, Fig. 2. The sequence begins in October 1992 (monsoon transition) with a northward intrusion of positive SLA through Socotra Passage into the GOA. It had an amplitude of 30 cm above the long-term mean, and maximum geostrophic surface velocity anomalies (not shown) of 70 and 120 cm/s on its western and eastern flanks, respectively. The timing and apparent origin (Socotra Passage) of this feature indicate that it is the 1992 SCR (Fratantoni et al., 2006). It is flanked to the east and west by areas of lower SLA. In mid-gulf (~49°E) is a second smaller positive SLA, with maximum amplitude of 5 cm and geostrophic surface velocity anomalies of 90 cm/s on its eastern flank. We have labeled this positive anomaly the Summer Eddy (SE) as it appears every summer in mid-gulf (see Section 3.3 for more details on the SE). West of the SE, in the far western GOA, SLA is relatively low.

During the following months of the winter monsoon, these anticyclones, woven together with cyclones, make up a train of five anomalies, which is joined by several more anomalies of alternating sign stretching east-northeastward from the gulf entrance. Through April 1993, these anomalies drift slowly westward deeper into the gulf. The SE becomes less distinct with time, SLA is increasing everywhere in the gulf and gradients are decreasing. Through April and May 1993 (monsoon transition), westward propagation is not as obvious, and two of the positive SLAs from the central Arabian Sea appear to merge and form one large area of positive SLA at the gulf entrance. The timing and location of this feature

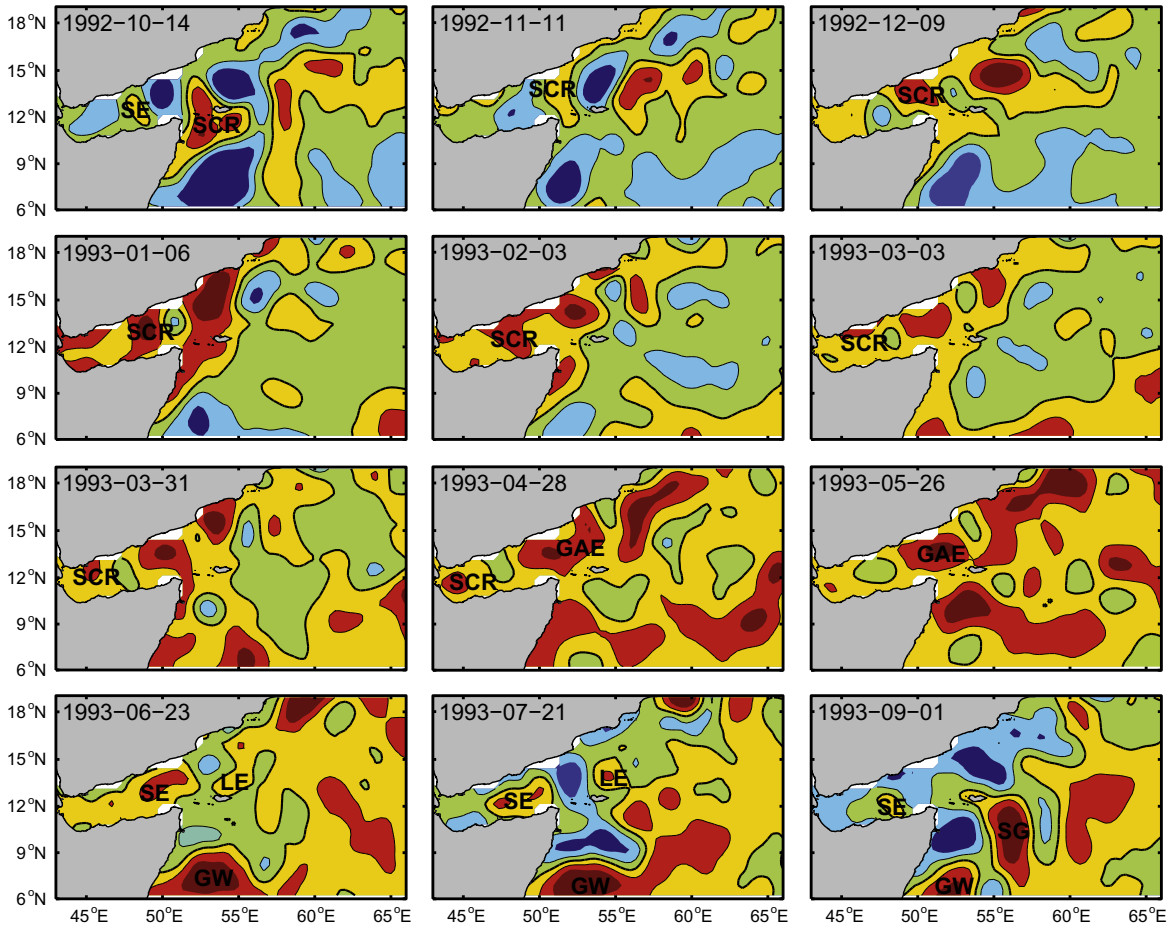

Fig. 2. Monthly time sequence of SLA (black contours) between October 1992 and September 1993. Contour interval is 5 cm; the bold black line marks the 0-cm contour interval, yellow and reds are positive SLA, and green and blue are negative SLA. Each panel is marked with the date of the SLA image, and with the named anticyclones or gyres: GAE – Gulf of Aden Eddy, GW – Great Whirl, LE – Lee Eddy, SCR – Somali Current Ring, SE – Summer Eddy, SG – Socotra Gyre.

indicate that it is the GAE described by Prasad and Ikeda (2001), although it is slightly farther west than usual during this year (see below). To the west, areas of negative and positive SLA persist through this time period.

In June and July (summer monsoon), an area of low SLA develops and deepens along the Somali east coast, through Socotra Passage and at the gulf entrance due to upwelling of colder water associated with the onset of the summer monsoon (Schott and McCreary, 2001). This appears to split the GAE, leaving two positive SLAs to either side, one in the GOA and the other north-northeast of Socotra Island. The former is the new SE; the remnants of the previous year's SE were evident in the first panel. The latter is hereafter called the Lee Eddy (LE), as it will be shown in Section 3.3 that it appears every year on the downwind (north) side of Socotra Island. Both of these positive anomalies persist through August, although they have shrunk in size and the amplitude of the LE has decreased substantially. Also during the summer monsoon, we see the development of the well-known Great Whirl and Socotra Gyre east of Somalia (see e.g., Schott and McCreary, 2001).

Fig. 3 shows the depth of the 20 °C isotherm (hereafter called z_{20}) in the GOA from the four AXBT surveys conducted during this time period, with contours of SLA on a date close to the middle of each survey superimposed. The 20 °C isotherm is in the middle of the main thermocline, as seen in the representative vertical temperature sections for each survey, Fig. 4. It ranges in depth, both spatially and temporally, from near the surface to about 150 m depth, and is visually well-correlated with the average depth of the main thermocline (16–25 °C). Temperature maxima below the thermocline are associated with relatively undiluted RSOW (Bower et al., 2000): they will be ignored for the purposes of this discussion.

The first important feature of these surveys to note is that there is significant seasonal variation in the average depth of z_{20} in the gulf. Comparison of the March and August 1993 surveys indicates that z_{20} is on average about 50 m shallower in summer (Figs. 3b, d and 5). As a result, the vertically averaged temperature over the upper 300 m is actually higher in winter (by about 2 °C) even though surface temperatures are higher in summer (by about 4 °C) (Fig. 4). The resultant steric height difference (about 9 cm) produces higher average SLA in winter and spring compared to summer and fall, as pointed out above and evident in Fig. 2. This seasonal cycle in thermocline depth and SLA, which is opposite of what would be expected from seasonal heating alone, has been attributed to monsoon winds, either in the GOA (Patzert, 1974) or in the Arabian Sea (Aiki et al., 2006).

The large-scale variations in z_{20} correlate well with high and low SLAs within each survey, Fig. 3. Depressions in z_{20} are typically associated with elevated SLA and represent warm anticyclonic eddies, and shallow z_{20} and lower SLA indicate cold cyclonic eddies, as will be shown with direct velocity observations in a later section. The named eddies identified in the monthly SLA sequence in Fig. 2 are also evident in z_{20}: the SCR and SE in the October 1992 survey, the GAE in the March 1993 survey, and another SE in the June and August 1993 surveys. Thermocline depth variations within one survey are as high as 100 m.

Some smaller eddies apparent in the z_{20} fields, mainly in the far western gulf, are not visible in SLA: this is not surprising in light of the relatively lower spatial resolution of the altimeter ground tracks (up to 300 km; see Section 2.3) during this time period. A good example is the cyclonic/anticyclonic pair in the southwestern gulf in the March 1993 survey. Below we will show that these smaller eddies that are undetectable with altimetry are critical in defining the initial spreading pathway of recently injected RSOW.

A Hovmöller diagram of SLA during 1992–1993, Fig. 6, serves as a useful summary of eddy appearance and progression (a 14-year Hovmöller diagram of SLA will be presented in Section 3.3 and Fig. 20). At the bottom of the diagram (October 1992), we see the SE and beginnings of the SCR, as well as the train of eddies of alternating sign stretching eastward from the entrance to the gulf. Between the October 1992 and March 1993 AXBT surveys, this train of eddies propagated westward at an average speed of approximately 7.4 cm/s. This is consistent with Al Saafani et al. (2007) estimate of the first baroclinic mode Rossby wave speed of 7.2 cm/s and his estimate from altimetric observations of 6.0–8.5 cm/s. The westward propagation of most eddies in the gulf persisted until about mid-April 1993 (monsoon transition), as also pointed out by Al Saafani et al. (2007). After that, eddies maintained their respective positions in the gulf. The GAE reaches maximum amplitude and zonal extent in early May 1993.

After the June survey, the positive SLA associated with the GAE is gradually replaced with an area of strong negative SLA at the entrance to the GOA, as also discussed by Al Saafani et al. (2007). This is due to very strong positive wind stress curl produced by an acceleration of the SW monsoon winds through Socotra Passage. What Al Saafani et al. (2007) did not point out however, is that this locally-forced elevation of the thermocline effectively splits the warm GAE in half, and both halves persist through the summer as smaller anticyclonic eddies. The western half, the SE, propagates slowly westward deeper into the gulf, and is the dominant anticyclonic feature there in the August 1993 AXBT survey, Fig. 3d. It is in approximately the same location as the SE observed at the beginning of the sequence in October 1992, Fig. 3a. The relatively weaker LE is also apparent in July. The area of strong negative SLA widens in longitudinal extent throughout the summer, and by the beginning of October covers almost all of the GOA.

3.1.2. 2001: Two CTD/LADCP surveys from REDSOX

The year of the REDSOX surveys exhibited some similarities and some differences to the 1992–1993 sequence of eddies described above. Fig. 7 shows the monthly sequence of SLA for the year including the REDSOX hydrographic surveys. In the Fall of 2000, when we would normally expect to see the SCR form as an intrusion of high SLA through Socotra Passage, an anticyclone is moving into the gulf north of Socotra Island (SCRa). It is not until January 2001 that a SCR forms by the typical process through the passage (SCRb). Al Saafani et al. (2007) documented a similar double-anticyclonic eddy structure which they argue is caused by the splitting of a larger high pressure eddy around Socotra Island. The positive and negative SLAs propagate westward into the gulf during the winter monsoon as described in the previous subsection for the AXBT year. As early as February 2001, the positive SLA that will become the GAE is forming near the Yemeni coast just outside the gulf. It grows in size and amplitude through May, and in June, the same splitting observed in 1993 begins, forming the SE to the west and the LE to the east. As before, the SE slowly drifts deeper into the gulf and the LE disappears through the summer. As also observed in 1993 (Fig. 2), the SE amplitude increases after it splits off the GAE: its surface currents are stronger on 4 July 2001 at about 48°E than it was when it first split off from the GAE in the 6 June 2001 image (Fig. 7).

In Fig. 8, SLA from 7 March 2001 and 29 August 2001 is superimposed on the pressure of the 27.0 σ_θ surface and the 300-m deep LADCP velocity vectors from REDSOX-1 and REDSOX-2. There is some clear visual correlation between SLA and the depth of the pycnocline, but some of the features observed during the *in situ* surveys are completely missing in SLA. For example, in March 2001, the deep thermocline at the eastern end of the survey area corresponds well to the positive SLA named SCRb, which emerged through Socotra Passage during January and propagated westward into the gulf (Fig. 8a; also see Fig. 7). The SLA also matches the deeper thermocline along the northern boundary of the gulf during

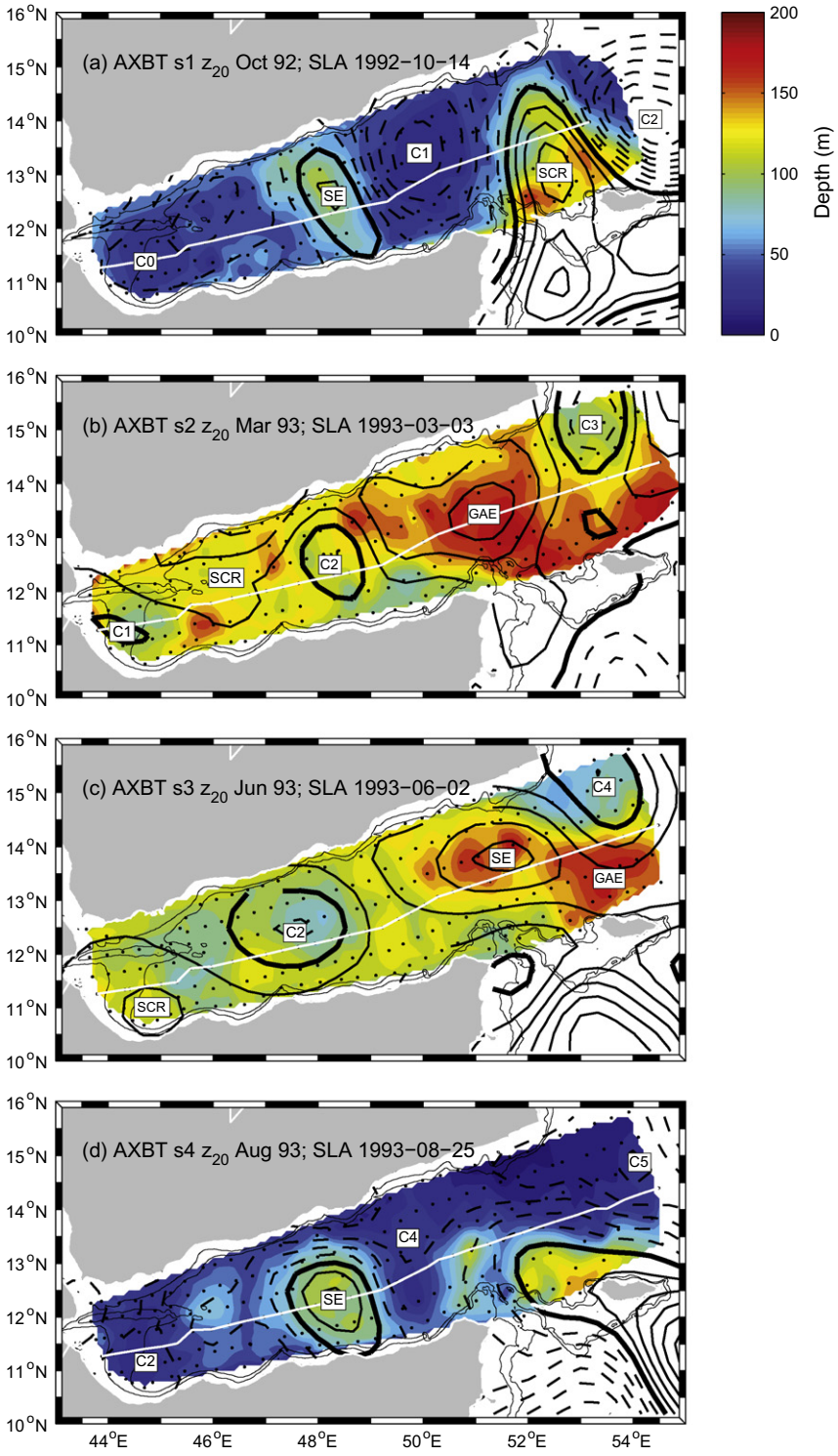

Fig. 3. Depth of the main thermocline, represented by the depth of the 20 °C isotherm (z_{20}) for four AXBT surveys conducted by NAVOCEANO in 1992 and 1993, see text for date ranges. Depressions are interpreted as warm, anticyclonic eddies, and shoaling as cold, cyclonic eddies. Coherent, identifiable anticyclones are labeled as in Fig. 2, and cyclones are labeled as 'C' and numbered sequentially. See text and later figures for more explanation. Dots are AXBT profile locations. Contour interval is 10 m, SLA data has been contoured over the AXBT data with a 5-cm contour interval; dashed lines are negative SLA, solid lines are positive, and the thick solid line is the 0-cm interval. White lines indicate the locations of sections shown in Fig. 4. The 500 and 1000 m isobaths are drawn as thin black lines.

REDSOX-1. What is not represented in SLA however is the shallow thermocline associated with a strong cyclonic eddy in the southwestern gulf during REDSOX-1. The SLA shows only a relatively flat sea surface in this region. In August (Fig. 8b), the positive SLA in the central gulf (the SE) corresponds well to a deeper thermocline and an anticyclonic circulation, but the cyclones to either side are not well-resolved in SLA.

While satellite altimetry has been used previously to investigate location and propagation of the larger eddy features in the gulf, the REDSOX observations offer the first look at their

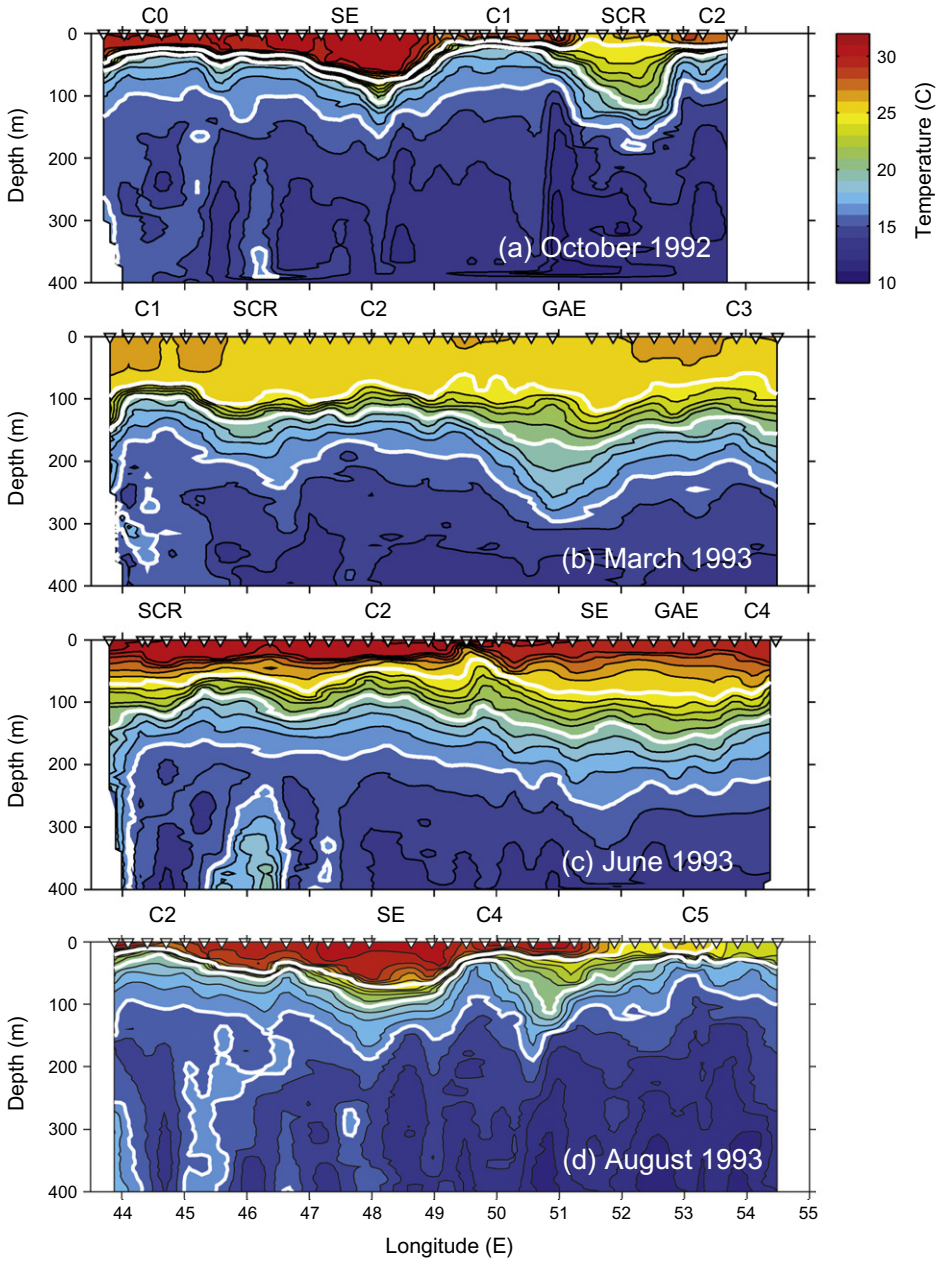

Fig. 4. Representative vertical temperature sections along the axis of the GOA for each of the AXBT surveys shown in Fig. 4, where white lines indicate section locations. The contour interval is 1 °C and the 25°, 20° and 16 °C isotherms, which span the main thermocline, are highlighted. Eddies identified in the previous two figures are labeled along the top of each panel.

subsurface velocity structure. Three cross-sections of zonal velocity from REDSOX-1, Fig. 9, show that the eddies often extend deep into the water column, including the depths at which RSOW equilibrates (indicated by the three isopycnals superimposed on the isotachs). The cyclone in the western gulf during REDSOX-1 is surface-intensified, with peak zonal velocities of 40–50 cm s^{-1}, Fig. 9a. Isopycnals at the RSOW levels bow upward near the center of the eddy, consistent with its cyclonic circulation and baroclinicity. At 46°E, Fig. 9b, an even more surface-trapped cyclonic eddy was observed with peak westward velocity near the northern gulf boundary of 50–60 cm s^{-1}. In contrast, the large anticyclone SCRb (48°E; Fig. 9c) has a *subsurface* velocity maximum of about 30–40 cm s^{-1} centered at about 350 m depth. It too extends to the depths of RSOW and deeper, and isopycnals are displaced downward at the center of the eddy. There is weak eastward flow near the southern boundary of the gulf in Fig. 9a and b at the RSOW depths, but this does not give the impression of a strong wall-bounded undercurrent as is observed in the case of the Mediterranean outflow (see e.g., Ambar and Howe, 1979a,b; Bower et al., 2005).

The sections of zonal velocity across the cyclone-SE-cyclone triplet observed during REDSOX-2, Fig. 9d–f, also show eddy velocities greater than 10 cm s^{-1} extending to (and beyond) the depths of RSOW. The SE, Fig. 9e, appears more surface-intensified and somewhat weaker than the cyclonic eddies on either side. Its currents do not penetrate as much into the depth range of RSOW.

Based on a preliminary analysis of the REDSOX-1 survey data only, Bower et al. (2002) argued that the eddies have a fundamental impact on the spreading pathways of RSOW through the GOA. Here we reinforce this point with a detailed analysis of both the REDSOX-1 and REDSOX-2 salinity distributions and LADCP velocity

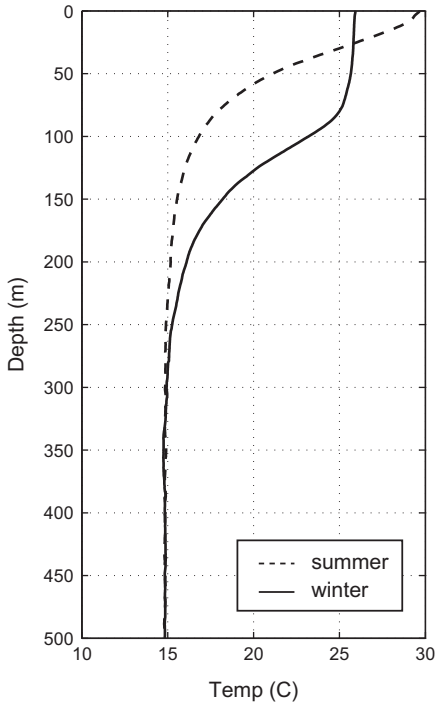

Fig. 5. Mean temperature profiles from the winter (solid line) and summer (dashed line) AXBT surveys, using data between 43 and 50°E. Mean surface temperature is higher in summer, but due to the much deeper thermocline in winter, the vertically-averaged temperature in the upper 300 m is higher in winter by about 2 °C.

vectors on the three density surfaces where the largest RSOW anomalies equilibrated (σ_θ = 27.0, 27.2 and 27.48; Bower et al., 2005), Fig. 10. During the winter survey, the highest salinities were found in the narrow Tadjura Rift at all three levels, Fig. 10a–c. Bower et al. (2005) already describe the vertical and horizontal salinity distribution in the rift, where the dense plumes of RSOW reach gravitational equilibrium. At the shallowest level, the escape of the outflow water from the rift and its advection around the cyclonic eddy in the southwestern GOA is clearly apparent, Fig. 10a. Low-salinity water at the core of the cyclone indicates that it has trapped and transported water from farther east to the far western gulf, setting up large salinity gradients in the western Gulf (35.7–35.8 in the eddy core compared to 36.8–36.9 in the surrounding streamer of outflow water). The transport of Indian Ocean water by eddies will be confirmed with the Lagrangian observations in the next section. The eddy has a larger radius near the surface than at depth (see Fig. 9a), suggesting that the edges of the eddy have been shaved off at depth as the eddy propagated into the southwestern corner of the gulf, following the narrowing channel of deeper water in that direction, and that the eddy has become more surface trapped over time as it travels the length of the gulf. Adjacent to the southeastern flank of the cyclonic eddy is a smaller detached patch of high-salinity water with anticyclonic circulation.

Interestingly, in a compilation of sparse historical salinity data in the GOA, Bower et al. (2000) noted a very similar vein of high-salinity outflow water following the continental slope south of the rift in a cyclonic fashion. They also showed in all the four synoptic AXBT surveys that the warmest (and presumably most saline) RSOW leaving the rift at 350 m was found south of the rift along the Somali coast, suggesting that the distribution observed during REDSOX-1 was not unique. What was not evident from the previous work but revealed with direct velocity observations is that a deep-reaching cyclonic eddy can cause the outflow water to follow the slope to the south of the rift. These observations are supported by the modeling study by Ilicak et al. (2011), where idealized RSOW from the Tadjura Rift was moved out of the gulf by a cyclonic eddy in a similar manner (see their Fig. 5). Ilicak et al. (2011) also demonstrate that when no eddies are present, the outflow preferentially develops cyclonic circulation, and adheres to the southern boundary of the gulf to about 47°E, conserving potential vorticity (Spall and Price, 1998).

East of about 46°E, salinity gradients on the shallowest density surface during REDSOX-1 were much weaker. Low-salinity water was found associated with the cyclonic eddy centered at 46–47°E and the anticyclonic eddy at 48°E. Fratantoni et al. (2006) pointed out that the 48°E eddy in this survey had a core of low salinity, low oxygen water above 400 m reflecting its origin in the tropical Indian Ocean and formation from a branch of the northward-flowing Somali Current through Socotra Passage. This is clearly appar-

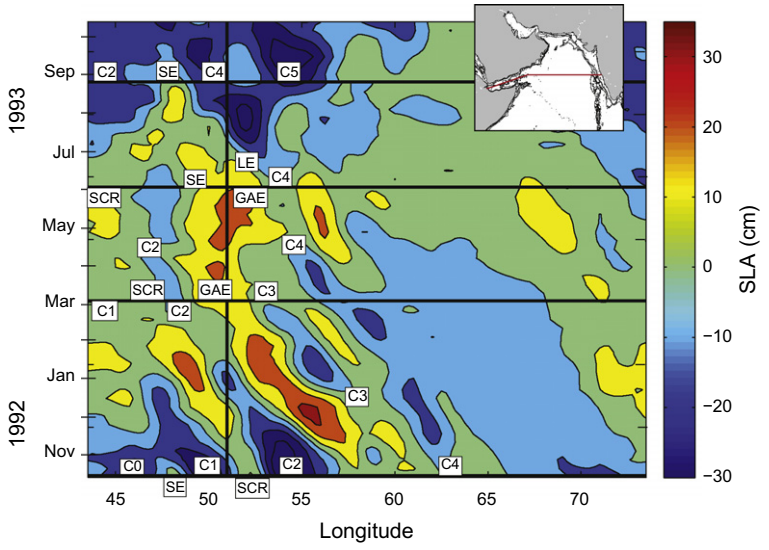

Fig. 6. Hovmöller diagram of SLA for the AXBT year 1992–1993. The data has been interpolated along the axis of the gulf to 51.5°E, then along the 14.5°N parallel, see inset. Contour interval is 10 cm; eddies have been labeled as in Figs. 2 and 3. The horizontal black lines mark when the AXBT surveys took place, and the vertical black line marked the change in direction of the Hovmöller line indicated in the inset figure, at about 51.5°E.

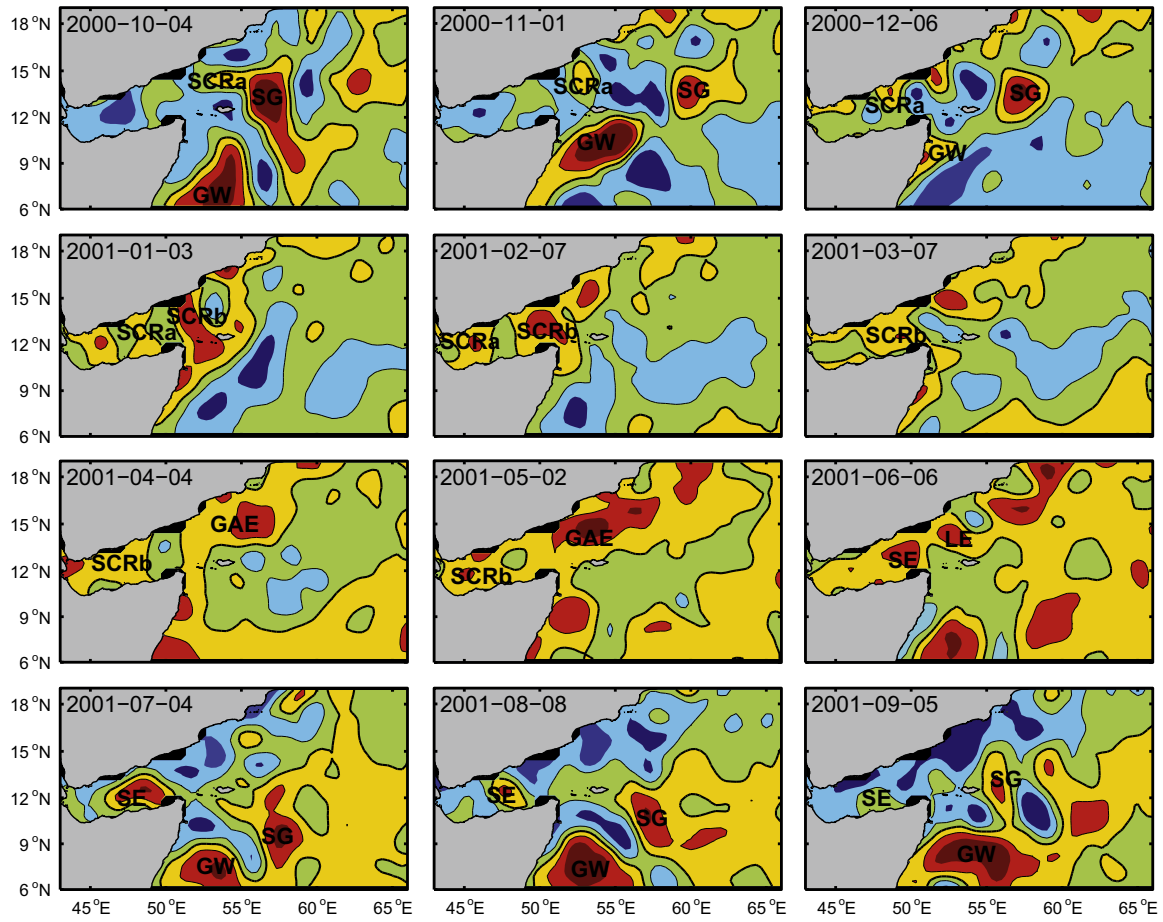

Fig. 7. Monthly time sequence of SLA between October 2000 and September 2001, the REDSOX year, presented as in Fig. 2. The panels dated 7 February 2001 and 8 August 2001 correspond most closely to REDSOX cruises #1 and #2, respectively.

ent in Fig. 10a. The cyclonic eddy whose core is located between 46° and 47°E (according to the LADCP vectors) is also coincident with low-salinity water, but its core properties were not measured during the survey. Higher salinity water was apparently being advected northward along 47°E between the central cyclone and eastern anticyclone and wrapping westward around the cyclone along the Yemeni coast.

The patterns at the middle density level are generally similar, Fig. 10b. Differences include a higher-salinity streamer that wraps more completely around the cyclone in the southwestern gulf, a better-defined small anticyclonic satellite eddy southeast of this cyclonic eddy, and higher average salinity and weaker lateral gradients in the central and eastern gulf. This figure shows convincingly that the RSOW is being advected around the cyclonic eddy in the southwestern corner, not following the isobaths along the Somali coast.

The deepest density surface, Fig. 10c, shows a very different salinity distribution in the western gulf. The strong cyclonic eddy so prominent at the upper surfaces was located higher up on the slope, and is not present at this depth (see Fig. 9a). The main vein of high-salinity RSOW was emerging from the Tadjura Rift, toward the east, likely steered by the underlying bathymetry of the rift (Fig. 1). Temperature at 800 m in the March 1993 AXBT survey shows a similar eastward tongue (Bower et al., 2000). The small anticyclonic eddy southeast of the cyclone is still evident in velocity, but little salinity anomaly is associated with it at this level. In the central and eastern gulf, the patterns are similar to what was observed at the upper surfaces: salinity gradients were generally weaker than in the west, patches of low-salinity water were found near the centers of the large cyclonic and anticyclonic eddies and diluted RSOW was being advected northward between the two eddies. The scale of the cyclone centered between 46° and 47°E seems to be set at this depth by the curvature of the 1500-m isobath north of the rift (see also Fig. 10b), indicating that it is being squeezed by the bathymetry.

The more restricted area surveyed during REDSOX-2 makes it difficult to trace the spreading pathways of RSOW through the gulf, but some important similarities and differences with the winter survey can be identified. Salinities in the western gulf were much lower than during winter, with a maximum of only 37.2 at the upper surface. Highest salinities in summer were more confined to the far western Tadjura Rift. As was found during the winter survey, the most saline water outside the rift was found south of the rift axis, and higher salinities were generally observed on the middle surface. In the central and eastern gulf, we generally see alternating bands of higher and lower salinities coinciding with the two cyclones there: diluted RSOW was apparently being advected northward along the eastern flank of each cyclonic eddy. Bower et al. (2000) showed a similar banded structure in temperature at the RSOW level in 1993, but its relationship to eddies in the gulf only becomes clear with the velocity observations from REDSOX. The anticyclonic SE did not extend to the depths of the RSOW (see Fig. 9e) and therefore does not appear to impact the spreading of RSOW. The streamer of relatively high salinity at 47°E includes a patch of salinity 36.6–36.7 (on the middle surface), higher than any salinities observed this far east during the winter survey. This patch is located southeast of the cyclonic eddy centered at 46.5°E, giving the impression that it has been advected around

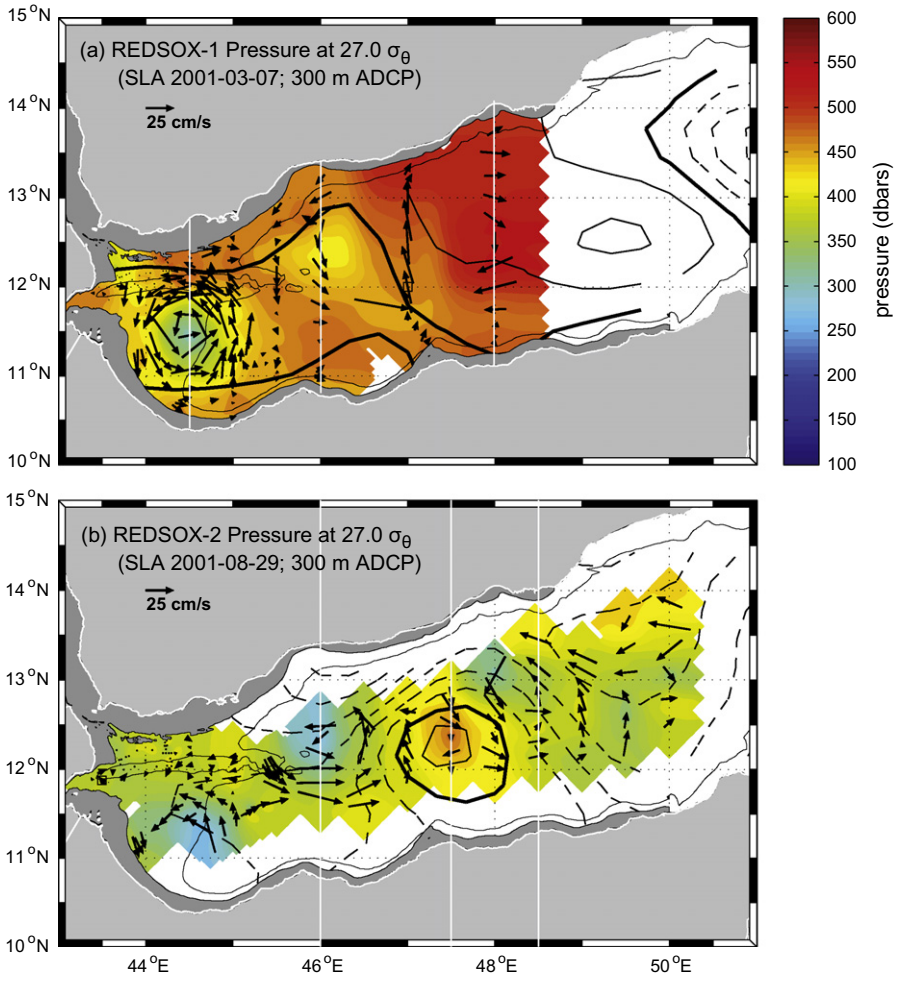

Fig. 8. Pressure of the 27.0 σ_θ surface for (a) REDSOX-1 (winter) and (b) REDSOX-2 (summer). SLA from a date within the survey time is contoured in black at 5 cm intervals, solid lines are positive SLA, dashed are negative, and the bold black line is the zero contour. Panel (a) has SLA from 7 March 2001, and panel (b) from 29 August 2001. LADCP velocity vectors at 300 m are drawn as black arrows. The three white meridional lines on each panel mark the locations of the vertical sections of velocity presented in the next figure.

its southern flank. A similar patch of high temperature outflow water was observed in the June 1993 AXBT survey (see Plate 5 in Bower et al. (2000)). At the deepest density surface, the northward advection of this streamer is not present: the western cyclone centered at 46.5°E is not as deep-reaching as the one farther east (see velocity vectors and Fig. 9d and f). The lowest salinity water in both surveys (35.2) was found at the eastern end of the gulf during the summer survey, which extended farther east than the winter survey.

These salinity and velocity maps reveal a consistent picture of how RSOW spreads through the GOA. The equilibrated RSOW, deposited in the Tadjura Rift mainly during winter, escapes from the rift and is advected around the periphery of mesoscale eddies that have propagated into the gulf from the Arabian Sea. This is most evident at the two shallower surfaces, but also at the deeper surface for the deepest-reaching eddies. Low-salinity water generally found in the centers of the eddies, even eddies found in the far western gulf, is apparently trapped when the eddies form outside the gulf and transport it completely through the gulf. This sets up a heterogeneous region in the western gulf with very large salinity gradients. Farther east in the gulf, salinity gradients are generally much weaker, reflecting the stirring action of the eddies and erosion of the salinity anomalies of the outflow.

Fig. 11 shows that the vertical profiles of salinity also vary significantly from west to east. In the top row are plotted salinity versus depth profiles from the winter and summer in the western, central and eastern gulf. The distribution of stations is shown in the lower row. In the western gulf, the individual winter salinity profiles are characterized by multiple layers of high-salinity RSOW between 100 and 1000 m depth, with maximum salinity > 39 at about 800 m (blue profiles in Fig. 11a). Some layering is still present 6 months later, but the maximum salinity values have been reduced to 38 and the shallowest intrusion of high-salinity water near 100 m is absent (red profiles in Fig. 11a; see also Bower et al., 2005, for a detailed description of equilibration depths of RSOW). The maximum mean salinities in winter and summer are similar, about 36.8, suggesting that the RSOW has been redistributed in the western gulf rather than diluted between the winter and summer surveys.

In the central and eastern gulf, the vertical structure of salinity is remarkably different in both summer and winter compared to the western gulf: the intrusions of very high salinity water have been mostly eroded by mixing and replaced by smoother profiles with a broad salinity maximum (Fig. 11b and c). One exception is the patch of relatively high salinity noted earlier near 47°E during summer (Fig. 9d and e), which has a maximum salinity of 36.6 centered at about 400 m. Peak mean salinities were similar in winter

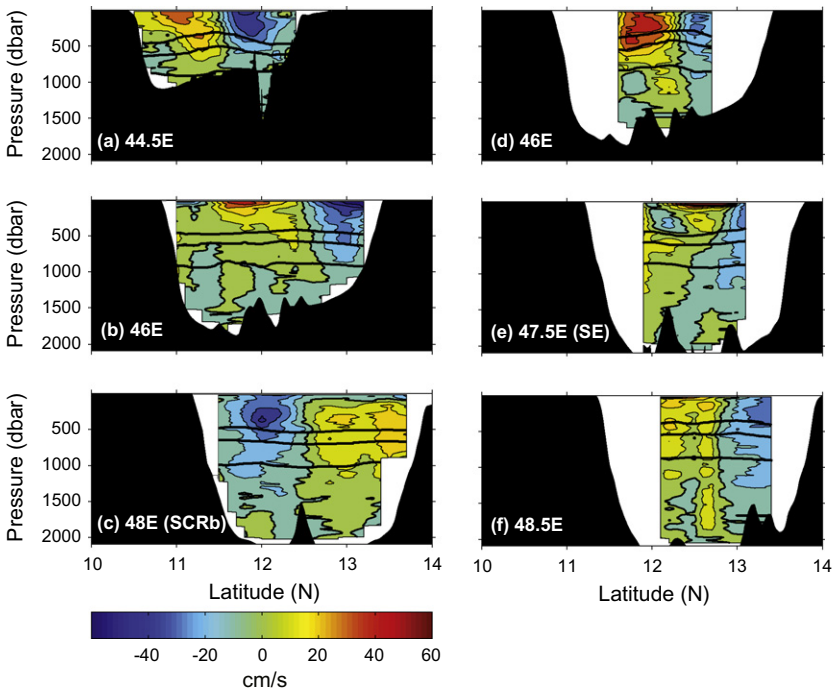

Fig. 9. Vertical sections of zonal velocity for REDSOX-1 (panels a–c) and REDSOX-2 (panels d–f). Locations of the sections are noted on each panel, and are drawn as white lines in Fig. 9. The bold black horizontal lines mark the locations of the density surfaces where RSOW salinity anomalies are highest (27.0, 27.2, and 27.48 σ_θ). Salinity on these same surfaces will be presented in Fig. 10.

and summer: about 36.2 in the central gulf and 35.9 in the eastern gulf.

3.1.3. Double-diffusive processes in the Gulf of Aden

We might expect that the mid-depth intrusion of warm, salty RSOW into the GOA sets up vertical temperature and salinity gradients that are favorable for double-diffusive mixing processes such as have been observed beneath MOW in the North Atlantic (e.g., Washburn and Kaese, 1987). Here we do not attempt to provide a comprehensive analysis of double-diffusive mixing in the GOA: there were no microstructure measurements made during the surveys and the topic is worthy of a dedicated study. Rather we show here with the 1-dbar averaged temperature and salinity profiles that conditions are strongly favorable for both salt fingering and diffusive convection and that there is direct evidence that both processes are active in the GOA. While the density ratio, $R_\rho = \alpha\Delta T/\beta\Delta S$, where α is the thermal expansion coefficient and β is the haline contraction coefficient, is often used to test for favorable conditions for double diffusion, here we use the Turner angle, defined as $(Tu = \tan^{-1}[(\alpha\Delta T - \beta\Delta S)/(\alpha\Delta T + \beta\Delta S)])$, a somewhat more practical means by which to determine where salt fingering (salt de-stabilizing) and double-diffusive layering (temperature de-stabilizing) may occur (Ruddick, 1983; Washburn and Kaese, 1987; Lillibridge et al., 1990). Here we use the sign convention of Washburn and Kaese (1987) (z-coordinate positive upward), in which case Turner angles from 0° to 45° indicate a water column that is unstable to salt fingering, although growth rates are fastest for Turner angles in the range 0–20° (R_ρ = 1–2.14; Schmitt, 1979; McDougall and Whitehead, 1984; McDougall and Taylor, 1984). Angles from 135° to 180° indicate a water column that is unstable to convective layering.

Fig. 12 shows profiles of Turner angle calculated using the mean temperature and salinity profiles from the western GOA in winter and summer (see Fig. 11a). Temperature and salinity gradients were estimated using the 1-dbar averaged CTD data at 1-dbar intervals by linear regression over a 10-dbar vertical scale. During winter, Fig. 12a, there are two layers that are unstable to double-diffusive mixing. From about 250–750 m, where the cooler, fresher Gulf of Aden Intermediate Water sits over the RSOW (Fig. 11a), convective layering is generally indicated, while at all depths below the RSOW salinity maximum (below ~1000 m), strong salt-fingering (Turner angles < 20°) is indicated, with minimum Turner angle immediately under the salinity maximum in the depth range 1000–1200 m (minimum density ratio of 1.3) and increasing gradually with increasing depth. The mean summer profile, Fig. 12b, is similar in that there is a layer generally conducive to convective layering overlying a deep layer unstable to strong salt fingering. In summer, a more well-defined layer of salt-fingering-favorable Turner angle is found centered at 600 m because there is a more pronounced salinity minimum there in the mean summer profile compared to winter. The basic structure of Turner angle shown in Fig. 12 is also found using mean temperature and salinity profiles from farther east in the GOA (not shown): the main difference going east is that Turner angles are somewhat larger below 1500 m, but still generally below 20°. The large depth range where the water column is favorable for double-diffusive processes suggests that salt fingering and convective layering may play an important role in redistributing heat and salt vertically in the gulf.

In fact, evidence of double-diffusive processes in the form of well-defined thermohaline staircases was observed in numerous CTD profiles in the Gulf. The most dramatic examples were found in a group of stations in the western Gulf during the summer survey, Fig. 13. Some well-mixed layers under the RSOW salinity maximum, in the depth range 800–1200 m, are 60-m thick (e.g., stations 144 and 145). Three layers appear to exhibit considerable spatial coherence over the group of stations (~50 km) when grouped by potential density (σ_1).

In an attempt to determine the temporal and horizontal extent of salt fingering activity throughout the survey area, we defined a steppiness index (following Washburn and Kaese, 1987), which is equal to the number of well-mixed layers below 300 m. A step was identified where a sharp negative salinity gradient (less than

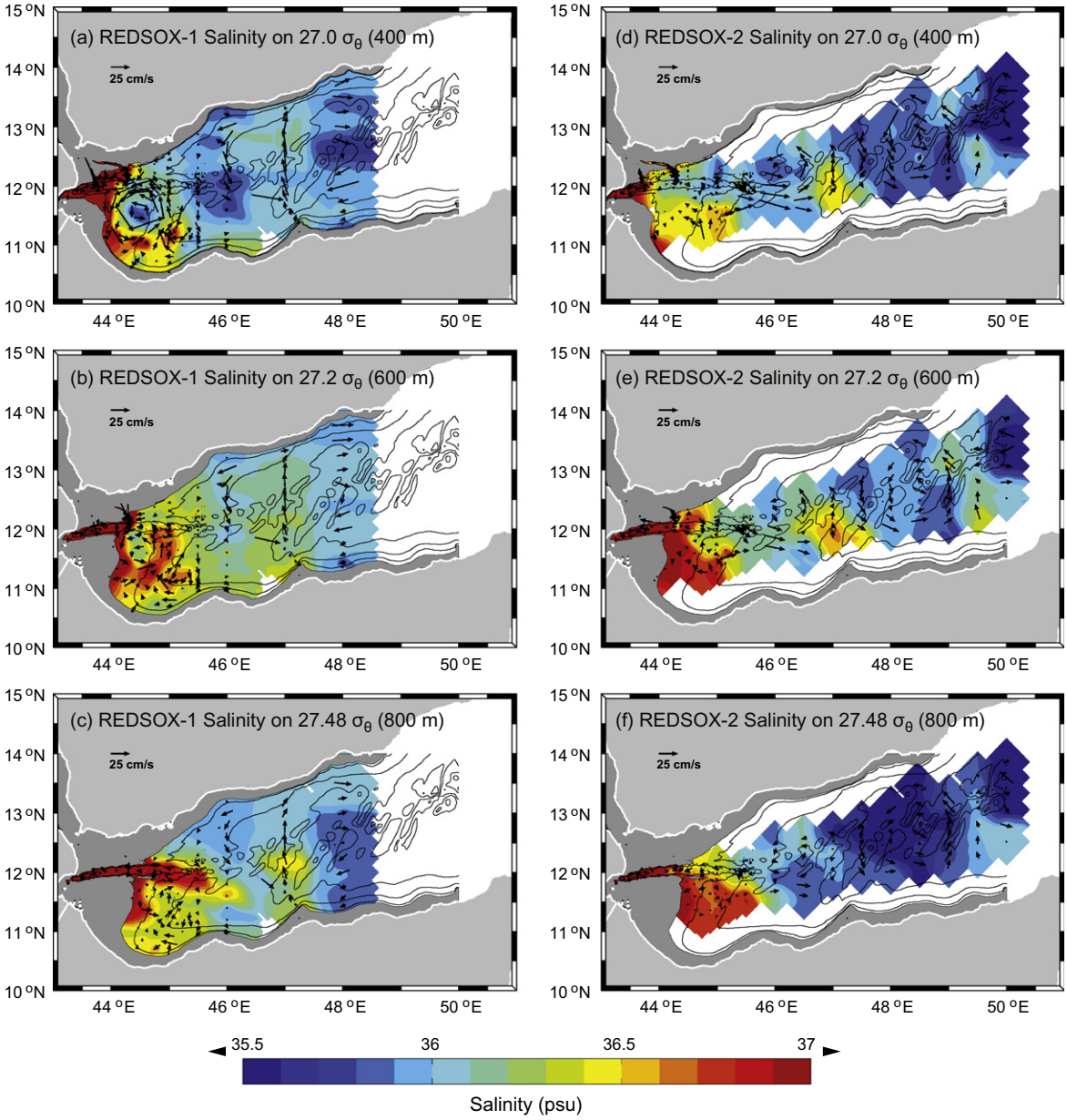

Fig. 10. Salinity on three density surfaces for REDSOX-1 (panels a–c) and REDSOX-2 (panels d–f). LADCP vectors are plotted as black arrows on each panel. (a and d) Salinity on the 27.0 σ_θ surface and LADCP vectors at 400 m; (b and e) salinity on the 27.2 σ_θ surface and LADCP vectors at 600 m; (b and e) salinity on the 27.48 σ_θ surface and LADCP vectors at 800 m.

−0.02/dbar) overlaid a well-mixed layer where the absolute value of the salinity gradient did not exceed 0.005/dbar for at least 10 dbar. These thresholds were determined by iteration and visual inspection of the profiles. An example of step identification for station 145 during the summer survey is shown in Fig. 14. A total of eight well-mixed layers that meet our criteria are marked, seven of them are below the deep salinity maximum at 800 m depth. This profile is remarkable also in that several well-mixed layers indicative of diffusive convection are observed above the deep salinity maximum, at least one with a thickness of about 30 m. These layers are not counted in the steppiness index, which only includes steps generated by salt fingering.

Fig. 15 shows the distribution of the steppiness index for the winter and summer surveys. The steppiest profiles were observed during summer (maximum number of steps below 300 m in one profile was 11, compared to 7 during winter). Profiles with the most steps (>5, black circles) are all found seaward of the 1000-m isobath: profiles in shallower water often had a salinity maximum near the bottom (i.e., no fresher/colder Indian Ocean Water below the RSOW). Comparing these maps to the salinity maps from the two surveys (Fig. 10), we see that the steppiest profiles are generally located at stations with the most saline RSOW. In winter, the steppiest profiles are associated with the veins of high-salinity water being swept into deep water by the cyclonic eddy in the southwestern corner of the Gulf and extending east-southeastward from the entrance of the rift. More steppy profiles were located at the southern end of the 47°E transect, where salinity is also elevated. In the summer survey, the profiles with the most steps are concentrated in the patch of high-salinity water in the southwestern gulf (see in particular Fig. 10f at 27.48 σ_θ). Little steppiness is

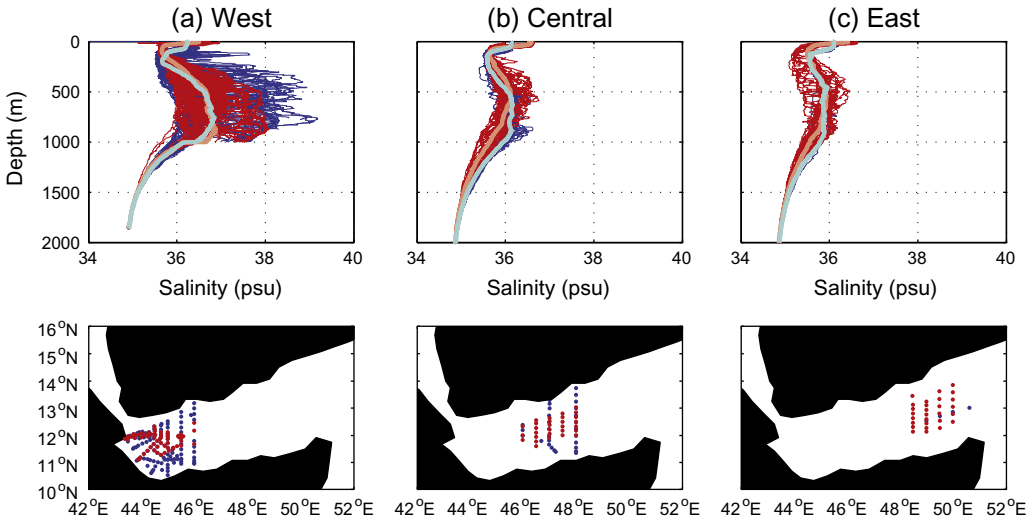

Fig. 11. West-to-east evolution of vertical profiles of salinity versus pressure. Top row shows individual salinity profiles, split by winter (blue, cyan) and summer (red, light orange) REDSOX cruises, for western (west of 46°E), central (46–48°E) and eastern (48–51°E) GOA. Bold lines show mean winter and summer profiles. Bottom row shows locations of stations used for the upper panels. Note that the *x*-axis limits in the upper and middle row are different.

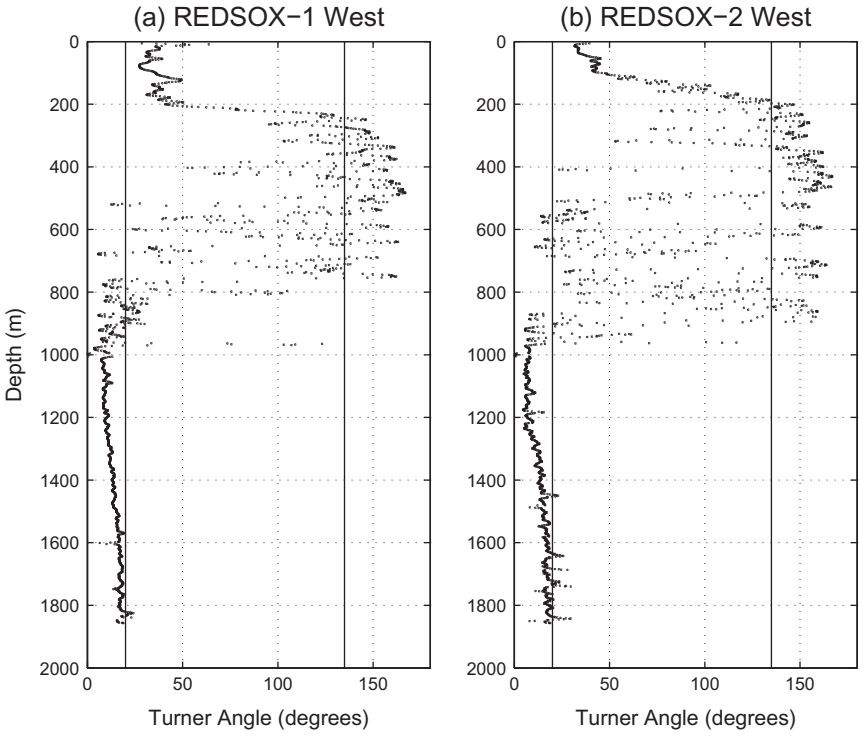

Fig. 12. Turner angle versus depth for (a) REDSOX-1 and (b) REDSOX-2, computed using the mean western profiles from Fig. 12. The solid vertical lines bounds the regions conducive to salt fingering (0–20°) and convective layering (135–180°).

observed over the Tadjura Rift because even though it is deeper than 1000 m, the 1000-m deep sill prevents the invasion of colder, fresher Indian Ocean Water into the deep rift. Unlike some regions of the World Ocean where the same well-mixed layers associated with salt fingering have been observed to persist for years and even decades (such as under the wide-spread Subtropical Underwater in the western North Atlantic (C-SALT area; Schmitt, 1994), the GOA layers shown here do not because the location and salinity of the small-scale intrusions of RSOW are altered by the eddies.

3.2. Lagrangian view of eddies

3.2.1. REDSOX floats 2001–2003: Overview and float examples

During the two REDSOX cruises in 2001, 53 floats were deployed on 1-year missions at 650 dbars, 34 from the research vessels during the cruises, and 19 between and after the cruises from 'float parks' (Zenk et al., 2000) on the sea floor (see Furey et al. (2005), for details). A total of 41 float-years of data were collected from February 2001 up to February 2003. The sound source array

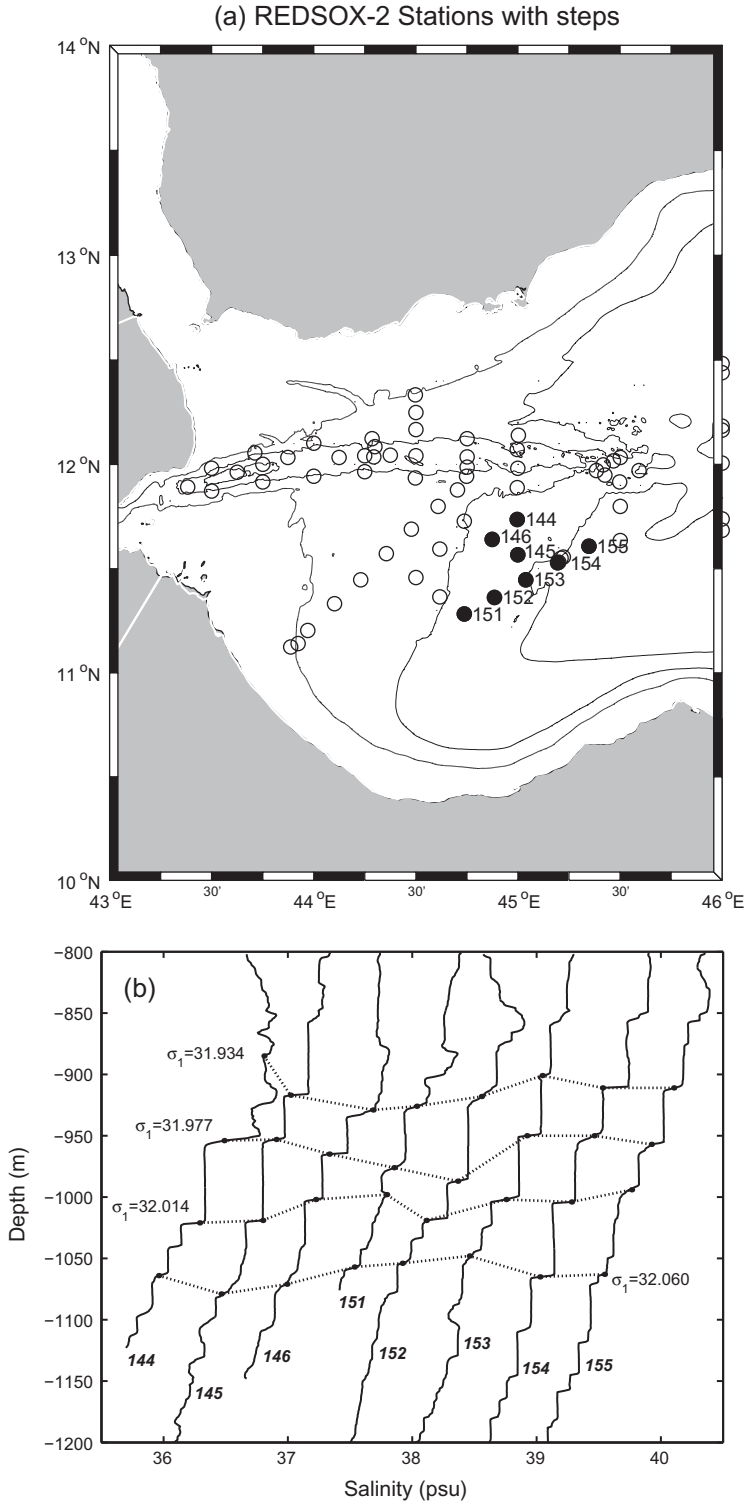

Fig. 13. (a) REDSOX-2 station locations (circles), where filled circles are for stations that contained steps in the salinity profiles. (b) Profiles from a group of stations in the western gulf that contained pronounced thermohaline staircases. Dotted lines show isopycnal depths and coherence of some layers over the group of stations.

design allowed floats to be tracked inside the GOA to about 52°E, and the majority of floats remained west of 52°E during the 2 year time period (Furey et al., 2005). Out of the 49 floats that surfaced and returned data, eight surfaced east of 52°E in the Arabian Sea: six to the northeast along the eastern Yemeni coast, and two to the southeast of Socotra Island.

Fig. 16 shows all the float trajectories (black), with trajectory segments slower than 10 cm/s marked in blue, and segments faster than 20 cm/s marked in red. The mean float speed, averaged in 1° wide bins, is plotted as a function of longitude on the inset plot, with one standard deviation error bars. The floats reveal that mid-depth circulation is dominated by eddy circulation that

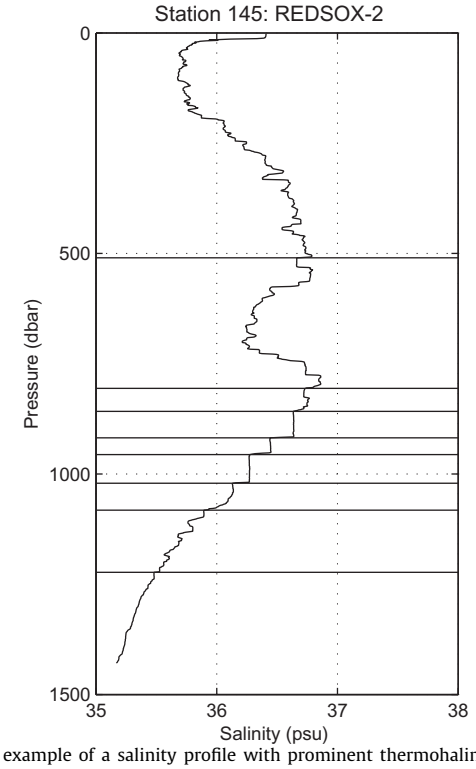

Fig. 14. An example of a salinity profile with prominent thermohaline staircases (REDSOX-2 station 145) illustrating steps identified with the criteria for calculating a steppiness index. The horizontal lines mark the location of the top of each step. The profile has some convective layering, but only salt fingering layers were counted for the steppiness index.

extends the width of the Gulf, similar to what has been shown in the LADCP data in the previous section (e.g., Figs. 8 and 9). Velocity is generally weakest in the western gulf and along the southwestern boundary, and faster in the central and eastern gulf, where large and energetic eddies stir the water, even at intermediate depths. The fastest speeds (red trajectory segments, Fig. 16) diminish west of about 45.5°E, at the eastern edge of the Tadjura Rift (Fig. 1). Mean float velocity and standard deviation increases from west to east, from 5.8 ± 4.1 cm/s to 15.9 ± 7.9 cm/s in the far eastern gulf (Fig. 16, inset). Formal mapping of the mean velocity was not carried out because the float trajectories were dominated by a small number (∼5) of westward-propagating gulf-scale eddies during the 2 year time period, making it impossible to define a mean field with any statistical confidence.

We have chosen two floats to illustrate the range of behaviors observed at 650 m in the GOA, float 146 that was trapped in the GOA for its entire 1-year lifetime and float 212 that escaped relatively quickly from the GOA and surfaced in the Arabian Sea. Fig. 17 shows the two floats: the left-hand column chronicles float 146, with the upper four left-hand panels showing the trajectory paired with SLA for four times during the floats mission, and float temperature presented on the bottom of the left-hand side. The right hand side depicts float 212 similarly. Both float trajectories were strongly influenced by the westward moving eddies present in the Gulf, with different outcomes.

Float 146 was deployed on the winter REDSOX-1 cruise and, as a delay-release float, began its mission 2 months later, on 1 May 2001. During its 1-year mission, It traveled through the Gulf from its launch position on the north slope of the Tadjura Rift at 12.0°N43.9°E (black dot, Fig. 17a), to its surface position in the northwest Gulf at 12.7°N45.7°E, on 30 April 2002, only about 200 km from its launch position. During the year, however, it traveled ∼4200 km in a circuitous path to the Gulf's entrance at 50°E and back to the west.

Float 146 spent the first four and a half months, May through mid-September, in the western Gulf, west of 45.5°E, crossing the Tadjura Rift from northwest to southeast, and slowly meandering in the southwest Gulf with speeds generally less than 5 cm/s (Fig. 17a). The float recorded temperatures > 19 °C at launch, falling to about 16 °C as it crossed over the rift, then rebounding to 17 °C after it entered the southwest Gulf, indicative of the heterogeneous distribution of water masses in the western gulf (Fig. 17e). After 4 months, the float was apparently entrained in a cyclone, as it was swept east and then north along the southeast edge of the cyclone. The float turned east, traveling a half-circle of what was probably a small O(50 km) diameter anticyclone. In November, five and a half months after launch, the water temperature drops abruptly from 17 to 14 °C over the course of 10 days (Fig. 17e, star marker on SLA plots and temperature record) as the float was entrained in a second cyclone for one and a half rotations, centered about 12.0°N46.5°E and about 200 km in diameter. The float then traveled quickly, at about 30 cm/s, anticyclonically across a region of positive sea level anomaly to the eastern Gulf (Fig. 17b), over the course of 7 days, making it to nearly 50°E before being entrained in a third cyclone. Fig. 17b shows the SLA on 12 December 2001, and during this period of travel from west to east, the SLA data does not correspond exactly to the float's movement below, though there is an anticyclonic feature centered at about 13.0°N48.5°E, the 2001 SCRa.

When float 146 neared the entrance of the Gulf it was entrained in a westward-traveling cyclone and remained in that cyclone for the rest of its mission, from January–May 2002 (Fig. 17c and d). The float velocities remained about 30 cm/s and temperatures at ∼14 °C, as the float made 14 complete loops with an average period of 8.75 days. During this time period, the altimetric data correlates well with the circulation at the float depth. SLA on 30 January 2002 (Fig. 17c), shows a strong (<−15 cm) negative SLA centered at 48.0°E and spanning the width of the Gulf, about 300 km in diameter. The float trajectory indicates that the float is traveling near the center of the cyclone between the 2001 SCRa and the 2001 SCRb at this point. The image two and a half months later (10 April 2002; Fig. 17d), shows the amplitude and diameter of the cyclone's SLA have diminished, with the anomaly less than −5 cm. The floats loops are also now much smaller in diameter, reduced from 110 km to 30 km, and centered in the northwest gulf, just east of the 1000-m isobath. Based on both the float loops and SLA maps, the cyclone appears to become smaller just as it encountered the sharply rising bathymetry of the eastern Tadjura Rift (see 1000 m isobath contour in Fig. 1). One other trajectory (see Furey et al., 2005) captured this type of event, with the gulf-scale eddy reducing diameter from 300 km to about 50 km just east of 46°E. Several studies have explored the interaction of submesoscale vortices with isolated topography, both using laboratory experiments (e.g., Cenedese, 2002; Dewar, 2002; Adduce and Cenedese, 2004), or with observations (float and CTD) data (e.g., Richardson et al., 2000; Bashmachnikov et al., 2009). An eddy-seamount collision may result in a drastic change in looping characteristics of an eddy and change in both temperature (Richardson et al., 2000) and salinity (Bashmachnikov et al., 2009) of the core properties. Eddies may split (Cenedese, 2002), become hetons (Hogg and Stommel, 1985), or may be destroyed (Richardson et al., 2000). In accordance with these studies, we surmise that the gulf-wide, westward traveling eddies are split or otherwise reduced in diameter when they are "impaled" on the rising seamounts at the eastern edge of the Tadjura Rift (Fig. 1). In this case, the looping diameter is reduced by 80 km over the course of less than one looping period (<8.75 days), and speeds decrease from ∼30 to 15 cm/s. There is no obvious

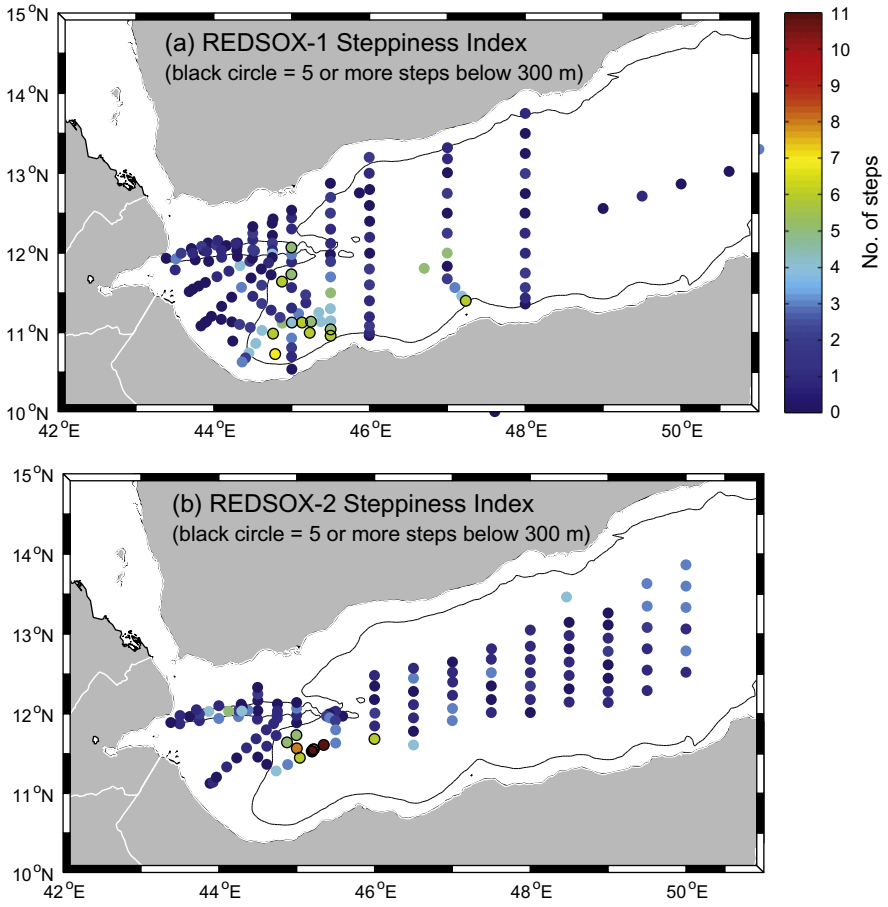

Fig. 15. The steppiness index for each station location in (a) REDSOX-1 and (b) REDSOX-2. Color gradient indicates number of steps, and stations with five or more steps below 300 m depth are rimmed with black.

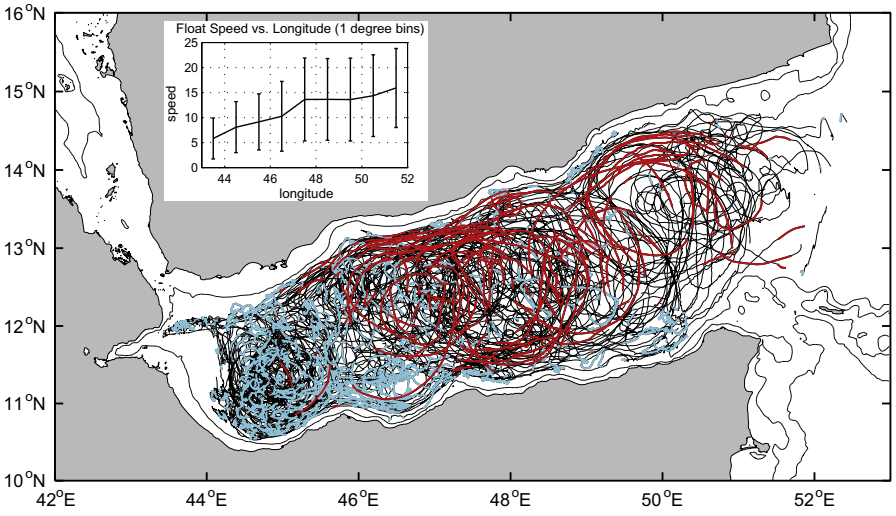

Fig. 16. All RAFOS float trajectories from REDSOX, smoothed using a 3-day Butterworth filter. Trajectories have been color-coded by speed as follows: speeds > 20 cm/s are drawn in red, <10 cm/s are blue, and between 10 and 20 cm/s are black. Float data has been culled to remove any float position data that was taken when a float was grounded. The 200 and 1000 m isobaths are drawn in thin black lines. Inset shows mean speed versus longitude for the float data binned in 1° longitude bands. One standard deviation error bars are plotted at each data point.

change in temperature, indicating that the float is still within the eddy core.

We also surmise that in these two cases, the eddies (or these eddy remnants) are then focused into a narrower basin to the northwest (45.5°E12.3°N), that they remain deep reaching (below the height of the seamounts and 1000 m isobath), thus their diameters are necessarily reduced to ~50 km. As we have seen previously in the CTD and LADCP data (Figs. 9 and 10), eddies with a

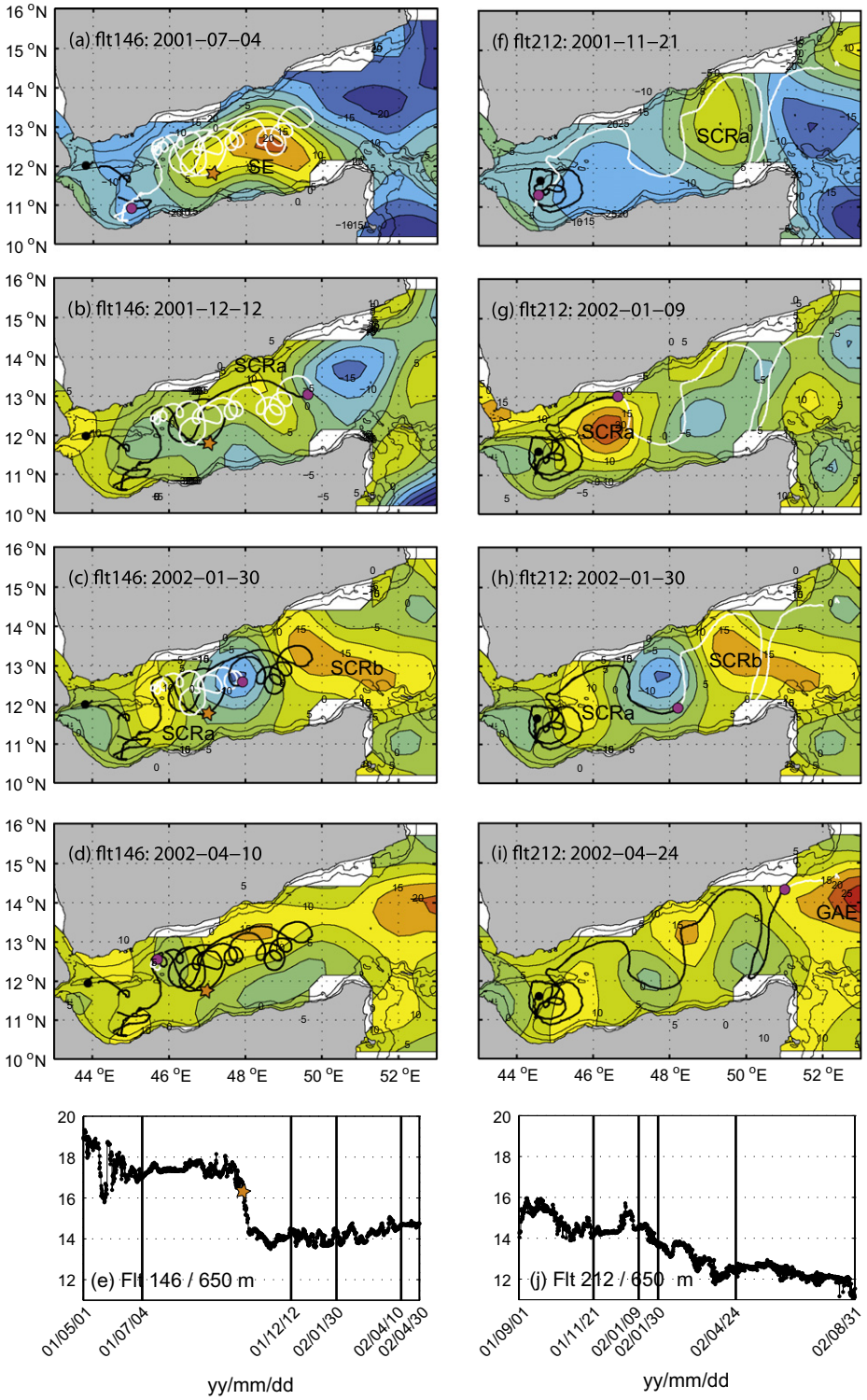

Fig. 17. Two float trajectories: left hand column, float 146 – a 'trapped' float, right hand column, float 212 – an 'escaped' float. The top four panels of each column show the float trajectory plotted on top of SLA images that correspond to the time the float is at the pink dot, with dates located in the upper left hand corner of each plot. The float trajectories have been color-coded as follows: Float launch location is a solid black circle, the position of the float on the title date is a pink dot. All previous track is in black, all future track is in white. SLA data is contoured and labeled at 5 cm intervals. The last panel in each column shows the temperature record for each float, with the dates of the images above marked as vertical black lines on the plots. On the left hand-column images for float 146, a star marks the position and date of the 3° temperature drop.

fresher/cooler core also travel into the southwestern basin west of 46°E where their deeper expression is similarly squeezed by the bathymetry. The effective trapping of water in the center of the cyclone results in the delivery of cool Indian Ocean water through the GOA and directly to the region where the much warmer RSOW is injected into the western GOA, creating very high lateral gradients in water properties (see Fig. 10, for example).

Float 212 (Fig. 17f–j) was deployed on the summer REDSOX-2 cruise south of the Tadjura Rift at 11.6°N44.6°E on 31 August 2001, and surfaced a year later outside the GOA at 12.9°N54.4°E,

a distance greater than 1100 km from the launch site. In contrast to the previous float example, the westward traveling eddies that entered the GOA served to transport this float, once entrained, quickly out of the gulf, in a period of 5 months.

Similar to float 146, float 212 spent the first 4 months (September through December) in the southwestern gulf (Fig. 17f). The float recorded temperatures that gradually decreased from 16 to 14 °C, well below the temperature of float 146, which was launched nearer the source of the RSOW and in the season with the highest outflow volume transport from the Red Sea (Bower et al., 2000). In January (Fig. 17g), the float is entrained by an anticyclone, in this case the SCRa. From there the float moves around the northern edge of the SCRa, cyclonically around the southern edge of the next eastward eddy – in this case a cyclone (the same cyclone that float 146 is trapped inside (Fig. 17c)), and then clockwise around the northern edge of the SCRb. The float slows its eastward (not meridional) progression a bit until the next anticyclone arrives. As the GAE intensifies, the float is then entrained (Fig. 17i) and moves clockwise to the north and out of the GOA.

The float's temperature record (Fig. 17j) steadily decreases from 16 to 13 °C from launch to the entrance to the GOA, then decreases to 11 °C once outside the gulf. This steady decrease, as compared to the 3 °C jump in temperature recorded by float 146, suggests steady mixing or diffusion of heat as the water parcel makes its way through the gulf. The temperature recorded by float 146, in contrast, drops suddenly. This float was launched into much warmer (19 °C) RSOW near the source (Tadjura Rift), and the temperature drop happens as the water parcel the float is embedded in becomes quickly mixed with the cold (14 °C) water of the cyclone centered at 46.5°E at that time. The water surrounding float 212 may also have been just as vigorously mixed as it was swept into the anticyclone centered at 46.5°E, but the weaker contrast in temperature made for a less dramatic record.

3.2.2. Horizontal temperature distribution recorded by 650-dbar floats

The large number of RAFOS floats present in the GOA from 2001 to 2003 provide an opportunity to study both the evolution of RSOW and the incoming Indian Ocean water using the temperatures recorded by the floats. Even though the RAFOS floats used in this experiment were isobaric, temperature changes along their trajectories are indicative of water mass changes and not just sloping isotherms (see Appendix). As shown in the previous section, float 146 recorded recently equilibrated water at 650 dbar having a temperature of 19 °C north of the Tadjura Rift, down to 17 °C after it crossed the rift (Fig. 17e). Float 212 (Fig. 17j) recorded water at the entrance to the gulf of ~12 °C. How and where does this water mix? The hydrographic and velocity data presented in Section 3.1 indicate that the RSOW is advected out of the GOA between the eddies, mixing along the way, and the float data reinforce this result.

Fig. 18a illustrates temperatures across the entire gulf at 650 dbars, from float data between 2–21 October 2001. At this time, floats from both cruises had been deployed, and in this example, 37 floats were in the water, spread across the gulf from the rift to about 52.0°E. SLA data from 10 October 2001 has been contoured over the temperature data. As was shown in the last section, float motion is often well correlated with SLA east of the Tadjura Rift (45.5°E), and this is corroborated in this image. SLA is relatively low throughout the GOA in Fall (Figs. 2 and 7), and the SLA in October 2001 is negative across most of the gulf. One strong cyclone is

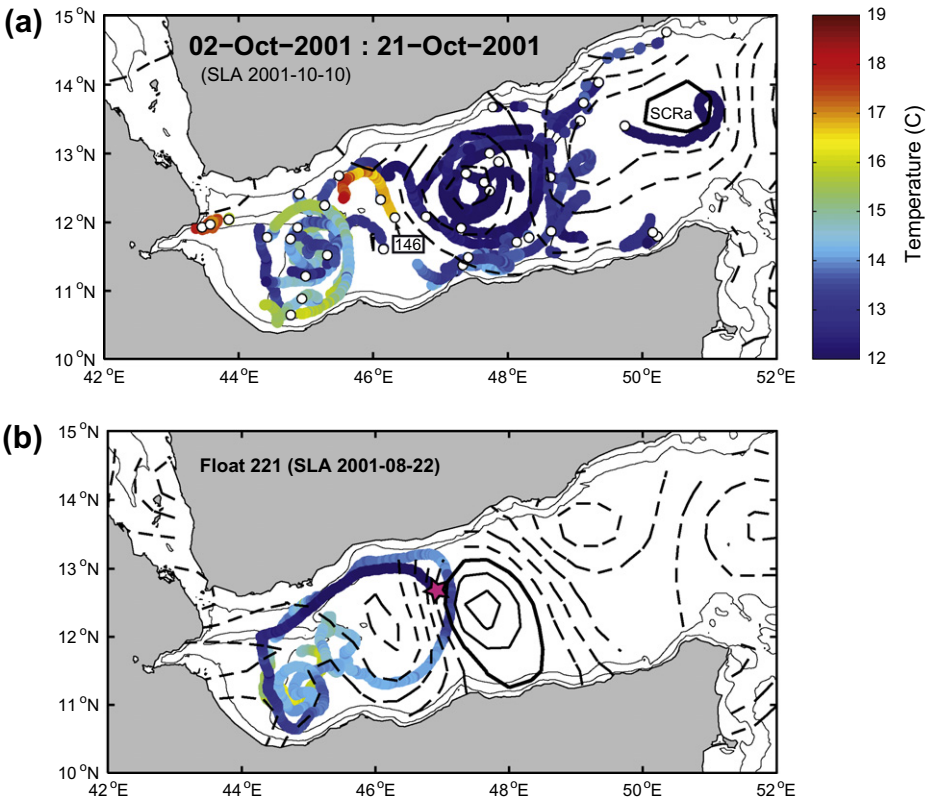

Fig. 18. (a) One three week period of float trajectories (2–21 October 2001) color-coded by temperature, illustrating the warmer temperature of recently injected RSOW, and the flow pattern at 650 dbars. Float position at the end of the time period (the 'head') is marked as white dots, edged by black. SLA data for 10 October 2001 has been contoured in black at 5 cm intervals, where dashed lines are negative, solid are positive. In this case, during the time when SLA across the region is relatively low, only a single 0-cm interval is visible at about 50.5°E. The segment for float 146 is marked on the plot. (b) A single 1-year float trajectory, color coded by temperature. SLA from 22 August 2001 is overlaid as in the panel above. The star marked the launch location of the float. Bathymetry for panels (a) and (b) are contoured at 200 and 1000 m depth.

present in the SLA data centered at 47.5°E, and an anticyclone, the SCRa, is depicted as a relative high to the east of the cyclone.

The trajectory segments indicate that the floats appear to be entrained in three eddies, a cyclone in the south western gulf centered at 45.0°E (not seen in the SLA), a second strong cyclone centered at 47.5°E, and the SCRa to the east. The float temperatures range from about 17.5 °C in the Tadjura Rift and between the two cyclones, down to 12 °C in the centers of the eastern cyclone and anticyclone. The temperatures are generally warmer on the edges of the eddies than in the center, consistent with the idea that the eddies transport cold water from outside the gulf westward into the gulf, and that outflow water from the Red Sea form filaments that skirt the edges of these eddies (Bower et al., 2002; Ilicak et al., 2011). This is also consistent with data we have previously presented (e.g., the CTD data, Fig. 10), where the RSOW is found along the edges of the eddies.

What is gained from studying the float data is that we can trace the source of the high temperature (and therefore high salinity; Bower et al., 2000) water directly back to the point of origin. One specific example: the single float trajectory segment measuring 16.5–17.5 °C water located at 46°E traces an anticyclonic pathway between the two cyclones, and this is the same float (146) discussed in the previous section (Fig. 17a–e). The temperature of this segment indicates its source is the RSOW, and following its path back (Fig. 17), we can see that this water parcel was originally tagged just north of the Tadjura Rift. This water parcel has remained relatively undiluted, and is moving out of the gulf on a path defined by the incoming eddies (and mixing along that path). This observation is supported by Ilicak et al. (2011).

Conversely, the westward traveling eddies transport the cold fresh water from the Indian Ocean into the GOA. Float 221 (Fig. 18b) was launched at 12.6°N47.0°E on 5 September 2001. The float was launched further east in the GOA than most of the other floats (launch location is marked as a star on the plot), between a cyclone and the SE. The SLA data, which is only relevant to the first week of the float's trajectory, show the cyclone and the eastward anticyclone, in this case the SE. The float measured its coldest temperature at launch, 12 °C. As it travels westward around the cyclone, it maintains its cold temperature until it reached the central Tadjura Rift, where the float turns due south and becomes entrained in a smaller scale cyclone (O(100 km)) for 2 months. Over this time, the float temperature gradually warms from 12 to 14 °C by December. The float is then kicked out into the central GOA, and is entrained again in another cyclone. The float registers slightly colder temperatures at is farthest extent east (13 °C), and then gradually warms again as in travels for a second time over the Tadjura Rift and into the southwest basin.

The longitudinal change in temperature distribution of all float data (Fig. 19) illustrates the position where the along-gulf temperature decreases are greatest. Temperature of all data is generally between 17–20 °C west of 44°E, east of this point the distribution of points broadens to 12–20 °C. The lower temperature limit remains about the same along the gulf, while the upper limit decreases eastward. The mean curve found from averaging the temperature data across 0.1° bins (thick black line, Fig. 19), shows two locations of greatest decrease, a 3° drop between 44.0 and 44.2°E and a 2° drop between 45.5 and 45.8°E. From about 44.0°E, the standard deviation decreases to the east. Although this represents a small number of independent realizations in time as compared to the annual cycle of eddies coming into the GOA (next section), the locations of the drops do suggest regions of intense mixing. The first drop is at the location of the recently equilibrated high temperature, high salinity RSOW in the Tadjura Rift. Standard deviation is relatively low in this location, as we expect from relatively homogenous water (thin black lines, Fig. 19). Floats at 650 dbars are constrained west of 44°E to the western Tadjura Rift, a receptacle for recently ventilated RSOW (Bower et al., 2005). (The temperature data points measuring less than 16 °C are confirmed by CTD profile data taken at the time of float launch – a 75 dbar intrusion of colder less saline water at this location, not shown.) The drop in mean temperature to the east of this location represents the geographic broadening of the float locations, and, circumstantially, the mixing that occurs once the RSOW leaves the rift. The standard deviation increases in this region, also reflecting the heterogeneous water. The second drop in temperature occurs at the eastern edge of the rift (45.5°E), where it was shown (Fig. 17, previous section) the large scale westward traveling eddies break apart into smaller scale eddies, and that float speeds are generally lessened westward (Fig. 16). The drop in temperature at this point suggests that this is a region of strong mixing, and the turbulence associated with the demise of eddies in this area is possibly the source of this mixing (again, circumstantially). As the mean temperature decreases east of 46.0°E, the standard deviation also decreases, indicating more homogenous water at the 650-m depth.

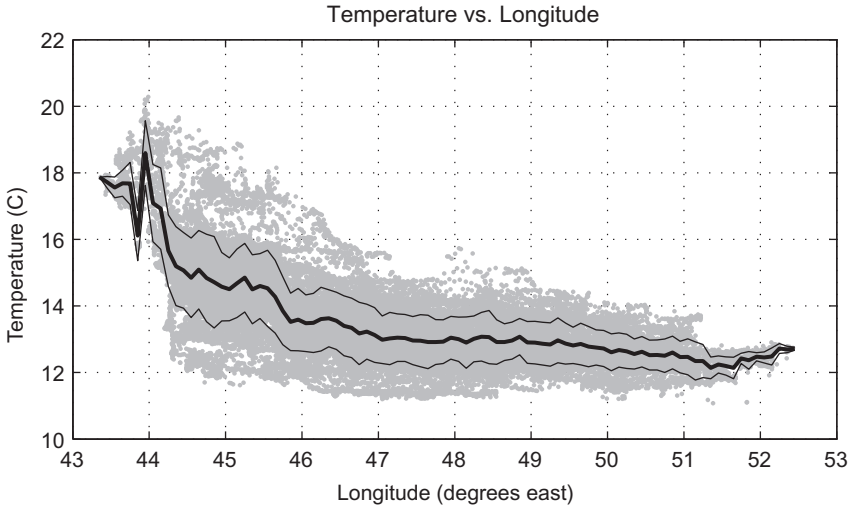

Fig. 19. All float temperature data plotted versus longitude. Mean temperature, averaged in 0.1° bins, is plotted as a thick black line, and the ±1 standard deviations are plotted above and below as thin black lines.

In the GOA, the eddies traveling westward from the Indian Ocean are the dominant means of mixing and define the pathways of RSOW transport out of the gulf. They are also the source for cold fresh water into the GOA. It is therefore important to understand the source and timing of these regularly occurring eddies.

3.3. Annual cycle in GOA eddies

In this section, we show that the sequence of large eddies observed in the GOA in 1992–1993 (Fig. 2) and 2001–2002 (Fig. 7) are more or less repeated every year with minor variations. Fig. 20 shows a Hovmöller diagram for the same section shown in Fig. 6, which stretches from the western GOA across the Arabian Sea to the coast of India, but for the entire 14-year SLA data set. A similar diagram was shown by Al Saafani et al. (2007), but here we will identify individual features in the western half of the diagram and the annual cycle in their appearance and movement as we attempt to bring together findings in the present study with those from earlier work.

One of the most striking aspects of the 14-year time series is the westward-propagating positive and negative anomalies in the eastern Arabian Sea (east of about 60°E), which have an annual period and propagation speed of approximately 7.9 cm/s. This feature has been noted in a number of earlier studies, and has been identified as an annual Rossby wave that originates off the west coast of India due to an annual cycle in wind stress curl there (e.g., Shankar and Shetye, 1997; Schott and McCreary, 2001; Brandt et al., 2002; Prasad and Ikeda, 2001; Al Saafani et al., 2007).

Of greater relevance to the present study is the annual cycle in the appearance, propagation and disappearance of the prominent anomalies in the western Arabian Sea and GOA. The SCR is the positive anomaly that appears nearly every year at about 52°E (the longitude of Socotra Passage), between October and January (Fratantoni et al., 2006). In some years, it begins propagating westward as soon as it appears at the entrance to the gulf (e.g., 1993) while in other years it remains stationary for 1–2 months before drifting westward deeper into the gulf (e.g., 2002 and 2003). It can typically be tracked through the gulf through March of the fol-

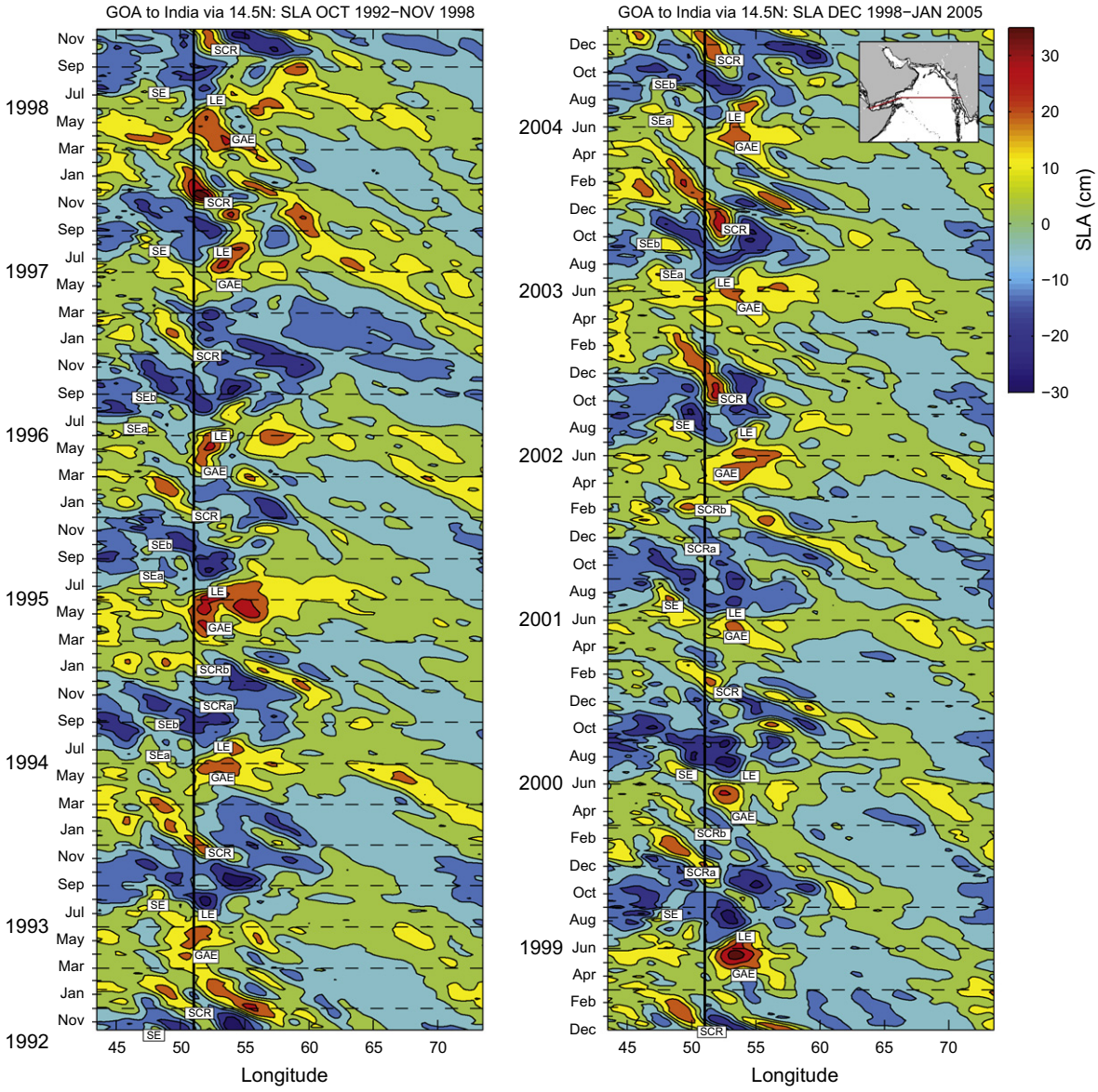

Fig. 20. Hovmöller diagram of SLA for the years 1992–2005. Left panel shows SLA versus time for October 1992 through November 1998. SLA data has been contoured at a 5 cm interval, with blues and greens negative, and yellows and red positive SLA. Right panel, same as left, but for the latter half of the time period: December 1998–January 2005. Inset shows Hovmöller 'line'. Data is presented as in Fig. 6, but only named anticyclones have been labeled.

lowing year (~5 months), and almost always to at least 47°E, and occasionally as far west as 45–46°E (e.g., March 1999 and March 2000; see also Fratantoni et al. (2006) who tracked eddies with SeaWiFS). Maximum SLA associated with the SCR can reach 35 cm above the long-term mean (e.g., November 2003). The SCR was weak and/or late appearing in 1994 and 2001 (the REDSOX year), and relatively strong SCRs occurred in 2002 and 2003.

Equally reliable in its annual appearance is the GAE (Prasad and Ikeda, 2001), in the longitude range 50–57°E, which begins to intensify in March–April each year and reaches maximum amplitude in May. In sharp contrast to the SCR, it does not propagate westward into the gulf as a whole. Rather it remains relatively stationary for up to 2 months (see also Prasad and Ikeda, 2001). The appearance of the GAE is sometimes preceded by one ore more westward-propagating features that appear to stall and form the GAE (e.g., 1993; see also Fig. 3). In most years, the maximum SLA of the GAE appears to shift slowly eastward through the summer, replaced at the gulf entrance by a developing negative SLA anomaly, as described for the year 1993 in Section 3.1.1 and by Al Saafani et al. (2007). New in this paper is that as the GAE amplitude decreases, the SE frequently breaks off its western flank and drifts deeper into the GOA. The SE intensifies after it enters the gulf, usually reaching maximum amplitude of up to 30 cm at 48°E (see Fig. 7 and below). Its life history and relationship to other mesoscale features has not been previously documented, although Fratantoni et al. (2006) briefly noted the re-occurrence of an eddy in six consecutive Septembers in altimetry at about 48°E. The eastern part of the GAE, the LE, is not always as visible, but some indication is present in nearly all years.

The SE is the most intense new eddy identified in the present study. It typically strengthens after it travels into the gulf (Fig. 21a), with the amplitude increasing until it reaches a maximum >+15 cm occurring at about 48°E, and usually in July (dates range from 5 July through 31 August for this 12-year period). The SE manifests itself both as a single anticyclone, as seen in the AXBT year (Fig. 2–4) and the REDSOX cruise year (Fig. 7), and occasionally as two anticyclones, SEa and SEb, as illustrated by the SLA images from summer 2003 (Fig. 21b). A single SE event typically begins with the anticyclone splitting off from the GAE in June, traveling westward in the GOA, intensifying through July, and then diminishing in amplitude as it travels west of 48°E. These changes in eddy amplitude may be related to the pattern of wind stress curl in the GOA during summer (see below). In a double SE event, the SE enters the gulf, intensifies in July, but then splits once inside the GOA into two anticyclones of similar amplitude (Fig. 21b). The westward eddy (SEa) diminishes in the western GOA, and the eastward eddy (SEb) moves westward, intensifying as it travels past 48°E (in the 2003 case, in September), and then weakens as it travels westward in the GOA.

The mean annual cycle in SLA is shown in Fig. 22 along with the monthly mean wind stress curl estimated from QuikScat winds for the years 2000–2006 (http://www.ssmi.com). The annual cycle in SLA accounts for 50–95% of the total variance in SLA in the GOA, Fig. 23. A similar sequence of the annual cycle in SLA was obtained from calculation of the annual and semiannual harmonics of SLA, but we choose to stick to the weekly mean in the middle of each month so as not to prematurely impose specific timing and periodicities.

Fig. 22 provides an effective summary of the timing and evolution of the major eddies in the GOA and their relationship to local wind forcing. Al Saafani et al. (2007) showed that the appearance of the strong negative LSA at the beginning of the summer monsoon is well-correlated with the local positive wind stress curl caused by the wind blowing strongly through Socotra Passage.

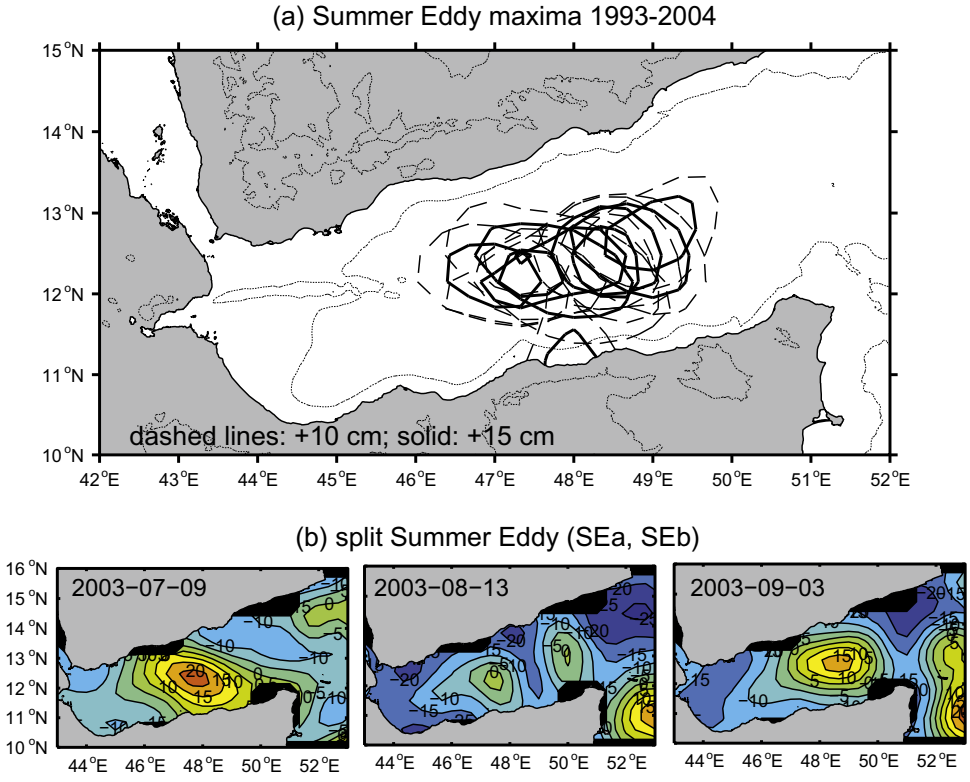

Fig. 21. (a) The position of the maximum SLA of the annual Summer Eddy (see text) for the years 1993–2004, maxima defined by the +15 cm contour interval. The +15 cm line is solid, and the +10 cm line is dashed. Bathymetry and topography are contoured at +1000 m, 0 m, and −1000 m. Note that the SE generally reaches maximum amplitude at about 48°E, usually in July. (b) A time sequence of SLA that shows an example of a split Summer Eddy (SEa, SEb), see text. The single SE corollary can be seen in Figs. 2 and 8.

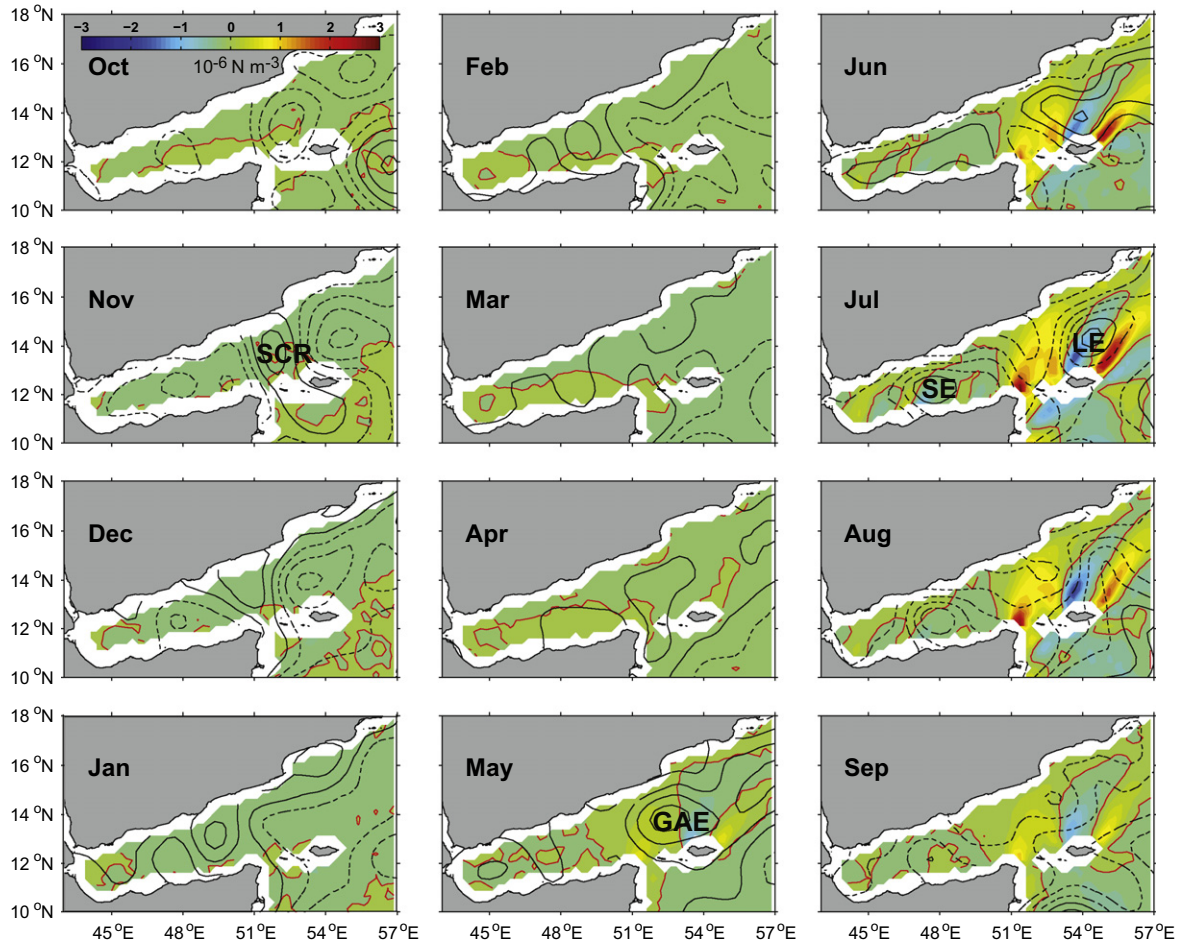

Fig. 22. Monthly plots of mean SLA, contoured in black as in Fig. 3, and the monthly mean wind stress curl from Quikscat for the years 2000–2004 (color shading) in units of 10^{-6} N m^{-3}. The mean SLA was computed from the 14-year time series by weekly averaging. The mean for a date near the middle of each month is shown.

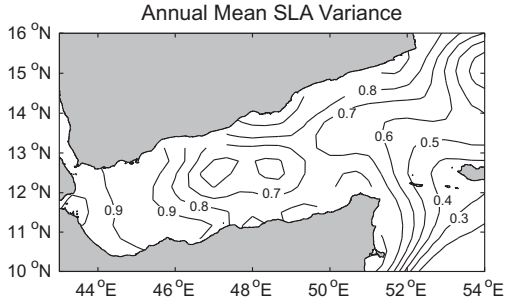

Fig. 23. Fraction of total variance explained by the mean annual SLA pattern shown in Fig. 22.

Fratantoni et al. (2006) showed the mean wind stress curl for the GOA in August 2000 and suggested the pattern of alternating positive and negative curl could lead to the generation of eddies in the mid-GOA. Here we show the monthly mean curl along with the annual cycle in SLA throughout the gulf region to provide a more complete picture of where and when local wind forcing may be important to eddy evolution. From October–February, the SCR appears through Socotra Passage and propagates westward in the gulf. The intrusion of warm water associated with the SCR effectively splits the large region of negative SLA that forms in the gulf during summer into two pieces, producing cyclonic neighbors for the SCR. From March–May, the GAE appears at the entrance to the gulf and increases in amplitude. Throughout these months of the winter monsoon, the wind stress curl is near zero. From June–August, banks of positive and negative wind stress curl form and strengthen where mountains in eastern Somalia and Socotra Island produce wind shadows for the strong southwest monsoon winds. By July, the GAE has been replaced by a region of low SLA, consistent with the positive curl and upwelling of colder water. To either side however, the positive-SLA SE and LE are situated under regions of negative wind stress curl which would tend to enhance their anticyclonic circulation through Ekman pumping. This could explain why the SE strengthens until it passes west of 47°E. The LE on the other hand disappears in August even though strong negative curl persists behind the western half of Socotra Island. The spatial scale of the curl pattern behind Socotra is likely reducing the scale of the eddies to one below detection by the altimeter ground tracks.

4. Discussion and summary

The Gulf of Aden is the receiving basin for one of the few high-salinity dense overflows worldwide, namely Red Sea Water, but almost nothing was known about its subsurface circulation and the spreading of equilibrated Red Sea Outflow Water through the gulf due to the lack of subsurface velocity observations. More is known about the spreading of RSOW as a mid-depth salinity maximum throughout much of the Indian Ocean than is known about the pathways and transformation of RSOW from its source at Bab al

Mandeb Strait through the GOA. Previous studies described the origin and propagation of some large, long-lived coherent eddies (diameters of at least 250 km, lifetimes up to 6 months) in the gulf based mainly on remote sensing observations (Prasad and Ikeda, 2001; Fratantoni et al., 2006; Al Saafani et al., 2007) and their potential to have a major impact on the spreading pathways of RSOW (Bower et al., 2002). In this paper, we have combined several extensive data sets collected during the Red Sea Outflow Experiment (REDSOX) in 2001 with historical AXBT surveys, satellite altimetry and the results from previous studies to provide a comprehensive view of the annual cycle in eddy activity and its impact on RSOW stirring and mixing. The new *in situ* data sets include two quasi-synoptic CTD/LADCP surveys at the peaks of the winter and summer monsoon seasons and trajectories from 49 acoustically tracked RAFOS floats, both of which reveal the depth-penetration of the eddies and their profound impact on RSOW.

The primary results of this study can be summarized as follows:

1. *Subsurface signature of sea level anomalies*: The basin-scale positive and negative SLAs frequently observed in the central and eastern GOA with amplitudes ±30 cm around the long-term mean are associated with ~100-m variations in the depth of the main thermocline and anticyclonic and cyclonic currents that extend deep into the water column. Most of the observed eddies were surface-intensified with azimuthal velocities as high as 50–60 cm/s at the surface and 20–30 cm/s at the depths of RSOW.
2. *Vertical and horizontal eddy scales smaller in the western GOA*: Smaller anticyclonic and cyclonic eddies (diameter ~100 km or less) also exist in the gulf, especially in the western gulf. These eddies are too small to be resolved with satellite altimetry, but they dominate the spreading of recently equilibrated RSOW in the western gulf. Some appear to be the remnants of larger eddies that have been cleaved into smaller eddies by the high topography of the Tadjura Rift.
3. *RSOW spreading pathways*: The highest salinities at the RSOW level were observed in the Tadjura Rift and in the southwestern gulf, indicating a preferred RSOW spreading pathway. Veins of high-salinity RSOW were observed to wrap around the eddies in the gulf, which typically have much lower salinities in their cores. In the western gulf, this generates exceptionally high lateral and vertical property gradients. East of about 46°E, property gradients on isopycnals are much weaker, suggesting rapid mixing of the RSOW with the background, although in general, higher salinities were found in the southern GOA and streamers of diluted RSOW were still observed wrapping around the fresher eddy cores here. The quickest route out of the Gulf recorded with these data were from a float that took 5 months to leave the GOA (cross 51°E) once entrained in an eddy (at ~45°E). This generally agrees with the estimate of Ilicak et al. (2011), where RSOW was transported from the Tadjura Rift to 48°E in bursts of less than 2 months, in that this float (Fig. 17, right hand column) took 2 months to cross 48°E, once entrained in an eddy. This suggests that, similar to the western Gulf from the Tadjura Rift to 48°E (the domain of the Ilicak et al. (2011) modeling study), RSOW is exported along pathways defined by the eddies, episodically. Seventeen per cent of floats were exported from the GOA in 1 year.
4. *GOA an active region of double-diffusive mixing*: Turner angles (related to density ratio) indicate that the whole water column below the layer of RSOW is strongly unstable to salt fingering throughout the GOA, and numerous profiles show evidence of thermohaline staircases, indicating that double-diffusive mixing processes are actively fluxing heat and salt. There is also some evidence of diffusive convection between the RSOW and fresher, cooler overlying GAIW. Staircases do not persist between the two REDSOX surveys, perhaps because of the strong time-dependence in the distribution of the RSOW and/or turbulence induced by the mesoscale eddy field, especially where it interacts with topography.
5. *Subsurface floats reveal eddy stirring in the GOA*: Float observations show relatively weaker velocities at the RSOW level (650 m) in the western gulf (~5 cm/s mean) compared to the eastern gulf (~15 cm/s mean). About 17% of the floats were exported from the GOA in 1 year (some within months of deployment); the rest circulated within the gulf for their entire mission, revealing the strong stirring action produced at depth by the mesoscale eddy field.
6. *Westward eddy transport of Indian Ocean Water*: Some floats were trapped within westward propagating eddies and revealed how cold Indian Ocean water is trapped and transported all the way to the western gulf by these eddies. This contributes to the rapid dilution of RSOW after it emerges from the Tadjura Rift.
7. *Annual cycle in major eddies in the GOA*: Others have shown previously that the SCR and GAE appear in the GOA more or less every year at the same time, and that the SCR propagates westward into the GOA while the GAE remains stationary. Here two more eddies have been added to the set of annually appearing mesoscale features, namely the Summer Eddy (SE) and the Lee Eddy (LE). These two eddies form at the beginning of the summer monsoon, when positive wind stress curl and rising thermocline at the entrance to the GOA split the warm GAE into two smaller anticyclonic eddies. The SE propagates westward into the GOA, often strengthening as it moves westward. While the generation of low SLA at the gulf entrance is aligned with the area of positive wind stress curl, the SE and LE both appear to be enhanced by negative wind stress curl (Ekman convergence) either inside the GOA (SE) or in the lee of Socotra Island (LE).

It is interesting to contrast the processes by which the product waters from the two best-known high-salinity overflows, namely the MOW and the RSOW, spread away from their respective sources. Both overflows descend along the sea floor after crossing over shallow sills: 160- and 300-m sill depth for the Red Sea and Mediterranean, respectively. The Red Sea overflow is more confined within bathymetric channels whereas the Mediterranean overflow is allowed to spread out more laterally over the continental slope, which has important implications for entrainment (e.g., Siedler, 1968; Bower et al., 2000; Peters et al., 2005; Matt and Johns, 2007;Price and O'Neil Baringer, 1994; Baringer and Price, 1997). After equilibration, the MOW continues to follow the continental slope as a wall-bounded jet all around the Iberian Peninsula (Ambar and Howe, 1979a,b; Daniault et al., 1994; Iorga and Lozier, 1999a,b) whereas the RSOW is deposited into the Tadjura Rift and does not appear to form a subsurface jet or undercurrent along the continental slope (this paper and Bower et al., 2005).

The Mediterranean Undercurrent frequently forms submesoscale coherent vortices containing a core of MOW that then separate from the slope and transport MOW sometimes thousands of kilometers westward and southwestward from the formation sites (see review by Richardson et al. (2000)). Many meddies have been discovered in the eastern North Atlantic and their physical properties and life histories have been well-documented (e.g., Armi and Zenk, 1984; Armi et al., 1989; Richardson et al., 1991; Zenk et al., 1992; Pingree and Le Cann, 1993; Prater and Sanford, 1994; Shapiro et al., 1995; Paillet et al., 2002; Serra and Ambar, 2002). It has been estimated that 8–20 of these so-called meddies may form each year (Richardson et al., 1989; Bower et al., 1997) and that they

may be responsible for 25% or more of the westward salt flux at mid-depth in the North Atlantic (Richardson et al., 1989; Maze et al., 1997). On the other hand, only one small anticyclonically rotating eddy with a core of RSOW was observed during REDSOX, adjacent to a larger cyclonic eddy in the southwestern GOA. Shapiro and Meschanov (1991) and Meschanov and Shapiro (1998) observed lenses of RSOW in the Arabian Sea, but based on the salinities in the cores of their lenses (35.20–35.85) these eddies apparently formed in the Arabian Sea, not in the GOA.

Based on the observations described in this paper, 'reddies' appear not to be important in the flux of RSOW through the GOA. There are at least three possible reasons: lack of a strong undercurrent, direction of monopole propagation on a β-plane and the presence of strong mesoscale eddies in the GOA. Several mechanisms have been proposed for the formation of meddies: separation of the Mediterranean Undercurrent from topography at a sharp corner (Bower et al., 1997), mixed baroclinic/barotropic instability of the undercurrent itself (Cherubin et al., 2000) and dipole formation as the undercurrent interacts with a deep canyon (Serra et al., 2005). With no undercurrent in the GOA, there seems to be no energy source to generate reddies. Even if a submesoscale lens of RSOW did form in the GOA, self-propagation dynamics dictate that it will propagate westward, i.e., back toward the high-salinity source. Finally, the location of the Red Sea outflow on a western, as opposed to eastern boundary also means much stronger mesoscale variability in the GOA compared to the eastern North Atlantic (e.g., Plate 8 in Ducet et al., 2000), which will likely shear a reddy apart soon after it formed and certainly before it managed to exit the GOA. The observations described in the present paper indicate that RSOW spreads away from its source primarily due to the stirring action of a vigorous mesoscale eddy field, which draws the outflow water out into narrow filaments where isopycnal and diapycnal mixing processes quickly diminish its thermohaline signature.

One question that has not been addressed in this study that could have wider implications is the role of the mesoscale eddies in the flux of heat and salt through Bab al Mandeb. The float and hydrographic data analyzed here showed that eddies formed outside the GOA are capable of trapping water at intermediate depths and transporting it to the western end of the gulf. With most of the eddies having surface-intensified velocity profiles, such trapping may be even more effective near the sea surface, resulting in the delivery of Arabian Sea water directly to the entrance to the Red Sea. This could also have an impact on the along-strait pressure gradient and exchange flow as the eddies modulate the stratification in the western gulf. Multi-year observations within the strait as well as at either end in the Red Sea and Gulf of Aden would be needed to investigate this further. Although it is beyond the scope of this paper, the large number of RAFOS floats in REDSOX make up a data set that is well-suited for a relative dispersion study.

Acknowledgements

The authors gratefully acknowledge the captains and crews of the *R/V Knorr* and *R/V Maurice Ewing*, and the shore-based vessel support staff at the Woods Hole Oceanographic Institution and the Lamont-Doherty Earth Observatory, for their assistance in obtaining the data analyzed here from a notoriously dangerous part of the world. This successful field program would also not have been possible without the many contributions of the REDSOX co-PIs (W. Johns, H. Peters and D. Fratantoni) as well as the engineers, technicians and analysts from the Woods Hole Oceanographic Institution and the Rosenstiel School of Marine and Atmospheric Science.

We also thank S. Swift (WHOI) and P. Huchon (Geosciences Azur) for their assistance in making the French multi-beam bathymetric data from the western Gulf of Aden available for our use, without which the REDSOX study would have been much more difficult. We also thank Dr. F. Pappirilla for early discussions about double diffusive mixing in the GOA: Fig. 13 was a result of those discussions during the second REDSOX cruise. The altimeter products were produced by the CLS Space Oceanography Division as part of the Environment and Climate EU ENACT project (EVK2-CT2001-00117) and with support from CNES. The authors would like to thank the anonymous reviewers for their suggestions for improving this study. This work was supported by grants to the Woods Hole Oceanographic Institution by the US National Science Foundation.

Appendix A

When showing temperature changes along the float tracks (Fig. 18), it is important to confirm that these differences are not due to the fact that the floats were isobaric rather than isopycnal. Temperature change on an isobar due to vertical displacement of isotherms can be estimated approximately from the average temperature gradient and typical vertical displacements of the isotherms. Fig. A1 shows the mean temperature profile in the GOA from the two hydrographic surveys and the results of a linear fit in the depth range 550–800 dbar. The vertical temperature gradient at the float depth was 0.0036 and 0.0051 °C/dbar for the winter and summer surveys, respectively. From the vertical sections in Fig. 9, isopycnals (proxy here for isotherms) vary in depth by ±50 m, giving a temperature difference on an isobar of 0.2–0.3 °C. This estimate is much smaller than the temperature changes observed along the float tracks (see text), indicating that those changes are mainly due to water mass differences and not the fact that the floats were isobaric.

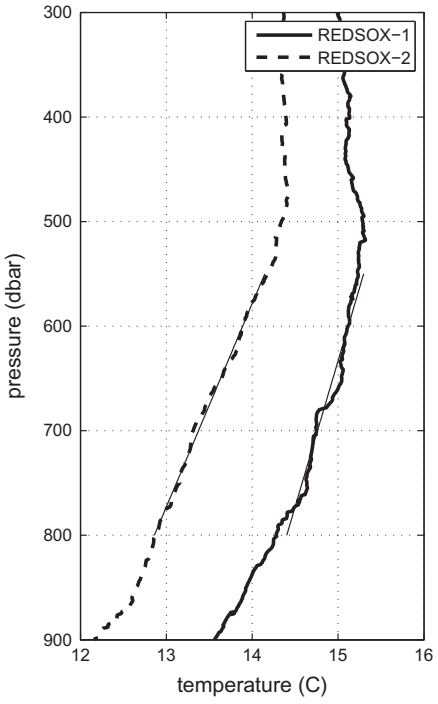

Fig. A1. The mean temperature profiles on the GOA from REDSOX-1 and REDSOX-2, plotted against pressure. The thin lines between 550 and 800 dbars are the linear fit to the data in that pressure range.

References

Adduce, C., Cenedese, C., 2004. An experimental study of a mesoscale vortex colliding with topography of varying geometry in a rotating fluid. Journal of Marine Research 62, 611–638.

Aiki, H., Takahashi, K., Yamagata, T., 2006. The Red Sea outflow regulated by the Indian monsoon. Continental Shelf Research 26, 1448–1468. doi:10.1016/j.csr.2006.02.017.

Al Saafani, M.A., Shenoi, S.S.C., Shankar, D., Aparna, M., Kurian, J., Durand, F., Vinayachandran, P.N., 2007. Westward movement of eddies into the Gulf of Aden from the Arabian Sea. Journal of Geophysical Research 112, @C11004. doi:10.1029/2006JC004020.

Ambar, I., Howe, M.R., 1979a. Observations of the Mediterranean outflow. 1. Mixing in the Mediterranean outflow. Deep-Sea Research 26, 535–554.

Ambar, I., Howe, M.R., 1979b. Observations of the Mediterranean outflow. 2. The deep circulation in the vicinity of the Gulf of Cadiz. Deep-Sea Research 26, 555–568.

Armi, L., Zenk, W., 1984. Large lenses of highly saline Mediterranean water. Journal of Physical Oceanography 14, 1560–1576.

Armi, L., Hebert, D., Oakey, N., Price, J.F., Richardson, P.L., Rossby, H.T., Ruddick, B., 1989. 2 Years in the life of a Mediterranean salt lens. Journal of Physical Oceanography 19, 354–370.

Baringer, M.O., Price, J.F., 1997. Mixing and spreading of the Mediterranean outflow. Journal of Physical Oceanography 27, 1654–1677.

Bashmachnikov, I., Mohn, C., Pelegri, J., Martins, A., Jose, F., Machin, F., White, M., 2009. Interaction of Mediterranean water eddies with Sedlo and Seine Seamounts, Subtropical Northeast Atlantic. Deep Sea Research Part II: Topical Studies in Oceanography 56, 2593–2605. doi:10.1016/j.dsr2.2008.12.036.

Beal, L.M., Ffield, A., Gordon, A.L., 2000. Spreading of Red Sea overflow waters in the Indian Ocean. Journal of Geophysical Research. C. Oceans 105, 8549–8564.

Bower, A.S., Armi, L., Ambar, I., 1997. Lagrangian observations of meddy formation during a Mediterranean undercurrent seeding experiment. Journal of Physical Oceanography 27, 2545–2575. doi:10.1175/1520-0485(1997)027<2545:LOOMFD>2.0.CO;2.

Bower, A.S., Hunt, H.D., Price, J.F., 2000. Character and dynamics of the Red Sea and Persian Gulf outflows. Journal of Geophysical Research. C. Oceans 105, 6387–6414.

Bower, A.S., Fratantoni, D.M., Johns, W.E., Peters, H., 2002. Gulf of Aden eddies and their impact on Red Sea Water. Geophysical Research Letters 29. doi:10.1029/2002GL015342.

Bower, A., Johns, W., Fratantoni, D., Peters, H., 2005. Equilibration and circulation of Red Sea Outflow Water in the Western Gulf of Aden. Journal of Physical Oceanography 35, 1963–1985. doi:10.1175/JPO2787.1.

Boyd, J.D., 1986. Improved Depth and Temperature Conversion Equations for Sippican AXBTs, NORDA Report 156, 6.

Brandt, P., Stramma, L., Schott, F., Fischer, J., Dengler, M., Quadfasel, D., 2002. Annual Rossby waves in the Arabian Sea from TOPEX/POSEIDON altimeter and in situ data. Deep-Sea Research Part II: Topical Studies in Oceanography 49, 1197–1210.

Cenedese, C., 2002. Laboratory experiments on mesoscale vortices colliding with a seamount. Journal of Geophysical Research. C. Oceans, 107. doi:10.1029/2000JC000599.

Chang, Y.S., Özgokmen, T.M., Peters, H., Xu, X., 2008. Numerical simulation of the Red Sea outflow using HYCOM and comparison with REDSOX observations. Journal of Physical Oceanography (38/2), 337–358.

Cherubin, L., Carton, X., Paillet, J., Morel, Y., Srpette, A., 2000. Instability of the Mediterranean Water undercurrents southwest of Portugal: effects of baroclinicity and of topography. Oceanologica Acta 23, 551–573. doi:10.1016/S0399-1784(00)01105-1.

Daniault, N., Maze, J.P., Arhan, M., 1994. Circulation and mixing of Mediterranean Water west of the Iberian Peninsula. Deep-Sea Research Part I: Oceanographic Research Papers 41, 1685–1714.

Dewar, W., 2002. Baroclinic eddy interaction with isolated topography. Journal of Physical Oceanography 32, 2789–2805. doi:10.1175/15200485(2002)032(2789:BEIWIT)2.0.CO;2.

Ducet, N., Le Traon, P.Y., Reverdin, G., 2000. Global high-resolution mapping of ocean circulation from TOPEX/Poseidon and ERS-1 and -2. Journal of Geophysical Research 105, 19477–19498. doi:10.1029/2000JC900063.

Fedorov, K.N., Meshchanov, S.L., 1988. Structure and propagation of the Red Sea water in the Aden Gulf. Okeanologiya/Oceanology 28, 357–363.

Fratantoni, D.M., Bower, A.S., Johns, W.E., Peters, H., 2006. Somali Current rings in the eastern Gulf of Aden. Journal of Geophysical Research. C. Oceans 111. doi:10.1029/2005JC003338,2006.

Furey, H.H., Bower, A.S., Fratantoni, D.M., Woods Hole Oceanographic Institution, 2005. Red Sea Outflow Experiment (REDSOX): DLD2 RAFOS Float Data Report, February 2001–March 2003. Woods Hole Oceanographic Institution, Woods Hole, Mass.

Hogg, N.G., Stommel, H.M., 1985. Hetonic explosions: the breakup and spread of warm pools as explained by baroclinic point vortices. Journal of the Atmospheric Sciences 42, 1465–1476.

Ilicak, M., Özgokmen, T.M., Peters, H., Baumert, H.Z., Iskandarani, M., 2008a. Very large eddy simulation of the Red Sea overflow. Ocean Modelling 20, 183–2006.

Ilicak, M., Özgokmen, T.M., Peters, H., Baumert, H.Z., Iskandarani, M., 2008b. Performance of two-equation turbulence closures in three-dimensional simulations of the Red Sea overflow. Ocean Modelling 24, 122–139.

Ilicak, M., Özgokmen, T.M., Johns, W.E., 2011. How does the Red Sea Outflow Water Interact with Gulf of Aden Eddies? Ocean Modeling 36, 133–148.

Iorga, M.C., Lozier, M.S., 1999a. Signatures of the Mediterranean outflow from a North Atlantic climatology 1. Salinity and density fields. Journal of Geophysical Research – Oceans 104, 25985–26009.

Iorga, M.C., Lozier, M.S., 1999b. Signatures of the Mediterranean outflow from a North Atlantic climatology 2. Diagnostic velocity fields. Journal of Geophysical Research – Oceans 104, 26011–26029.

Johns, W., Peters, H., Zantopp, R., Bower, A.S., Fratantoni, D.M., 2001. CTD/O2 Measurements Collected Aboard the R/V Knorr, February–March 2001: REDSOX-1. University of Miami, Miami, FL.

Le Traon, P., Dibarboure, G., 1999. Mesoscale mapping capabilities of multiple-satellite altimeter missions. Journal of Atmospheric and Oceanic Technology 16, 1208–1223. doi:10.1175/1520-0426(1999)016<1208:MMCOMS>2.0.CO;2.

Lillibridge III, J., Hitchcock, G., Rossby, T., Lessard, E., Mork, M., Golmen, L., 1990. Entrainment and mixing of shelf/slope waters in the near-surface Gulf Stream. Journal of Geophysical Research. C. Oceans 95, 13065–13087.

Matt, S., Johns, W.E., 2007. Transport and entrainment in the Red Sea outflow plume. Journal of Physical Oceanography 37, 819–836. doi:10.1175/JPO2993.1.

Maze, J.P., Arhan, M., Mercier, H., 1997. Volume budget of the eastern boundary layer off the Iberian Peninsula. Deep-Sea Research Part I: Oceanographic Research Papers 44, 1543–1574.

McDougall, T., Taylor, J., 1984. Flux measurements across a finger interface at low values of the stability ratio. Journal of Marine Research 42, 1–14.

McDougall, T.J., Whitehead, J.A., 1984. Estimates of the relative roles of diapycnal, isopycnal and double-diffusive mixing in Antarctic Bottom Water in the North Atlantic. Journal of Geophysical Research 89 (C6), 10479–10483.

Meschanov, S.L., Shapiro, G.I., 1998. A young lens of Red Sea water in the Arabian Sea. Deep-Sea Research Part I: Oceanographic Research Papers 45, 1–13.

Murray, S.P., Johns, W., 1997. Direct observations of seasonal exchange through the Bab el Mandab Strait. Geophysical Research Letters 24, 2557–2560.

Ozgokmen, T.M., Johns, W., Peters, H., Matt, S., 2003. Turbulent mixing in the Red Sea outflow plume from a high-resolution nonhydrostatic model. Journal of Physical Oceanography (33/8), 1846–1869.

Paillet, J., Le Cann, B., Carton, X., Morel, Y., Serpette, A., 2002. Dynamics and evolution of a Northern Meddy. Journal of Physical Oceanography 32, 55–79.

Patzert, W.C., 1974. Volume and Heat Transports between the Red Sea and Gulf of Aden, and Notes on the Red Sea Heat Budget. CNEXO, Paris, France.

Peters, H., Johns, W., 2005. Mixing and entrainment in the Red Sea Outflow Plume. II. Turbulence characteristics. Journal of Physical Oceanography 35, 584–600.

Peters, H., Johns, W., Bower, A.S., Fratantoni, D.M., 2005. Mixing and entrainment in the Red Sea Outflow Plume. I. Plume structure. Journal of Physical Oceanography 35, 569–583.

Pingree, R., Le Cann, B., 1993. Structure of a meddy (Boddy 92) southeast of the Azores. Deep-Sea Research Part I: Oceanographic Research Papers 40, 2077–2103.

Prasad, T.G., Ikeda, M., 2001. Spring evolution of Arabian Sea High in the Indian Ocean. Journal of Geophysical Research 106, 31085–31098. doi:10.1029/2000JC000314.

Prater, M.D., Sanford, T.B., 1994. A Meddy Off Cape-St-Vincent. 1. Description. Journal of Physical Oceanography 24, 1572–1586.

Price, J.F., O'Neil Baringer, M., 1994. Outflows and deep water production by marginal seas. Progress in Oceanography 33, 161–200.

Richardson, P., Walsh, D., Armi, L., Schroeder, M., Price, J., 1989. Tracking three meddies with SOFAR floats. Journal of Physical Oceanography 19, 371–383.

Richardson, P., McCartney, M., Maillard, C., 1991. A search for meddies in historical data. Dynamics of Atmospheres and Oceans 15, 241–265.

Richardson, P.L., Bower, A.S., Zenk, W., 2000. A census of meddies tracked by floats. Progress in Oceanography 45, 209–250.

Rossby, H.T., Dorson, D., Fontaine, J., 1986. The RAFOS system. Journal of Atmospheric and Oceanic Technology 3, 672–679.

Ruddick, B., 1983. A practical indicator of the stability of the water column to double-diffusive activity. Deep-Sea Research 30, 1105–1107.

Schmitt, R.W., 1979. Growth-rate of super-critical salt fingers. Deep-Sea Research 26, 23–40.

Schmitt, R.W., 1994. Double-diffusion in oceanography. Annual Review of Fluid Mechanics 26, 255–285.

Schott, F., McCreary Jr., J., 2001. The monsoon circulation of the Indian Ocean. Progress in Oceanography 51, 1–123.

Serra, N., Ambar, I., 2002. Eddy generation in the Mediterranean undercurrent. Deep-Sea Research Part II: Topical Studies in Oceanography 49, 4225–4243.

Serra, N., Ambar, I., Käse, R.H., 2005. Observations and numerical modelling of the Mediterranean outflow splitting and eddy generation. Deep Sea Research Part II: Topical Studies in Oceanography 52, 383–408. doi:10.1016/j.dsr2.2004.05.025.

Shankar, D., Shetye, S.R., 1997. On the dynamics of the Lakshadweep high and low in the southeastern Arabian sea. Journal of Geophysical Research – Oceans 102, 12551–12562.

Shapiro, G., Meschanov, S., 1991. Distribution and spreading of Red Sea water and salt lens formation in the northwest Indian Ocean. Deep Sea Research Part A: Oceanographic Research Papers 38, 21–34.

Shapiro, G.I., Meschanov, S.L., Emelianov, M.V., 1995. Mediterranean lens "Irving" after its collision with seamounts. Oceanologica Acta 18, 309–318.
Siedler, G., 1968. Schichtungs und Bewegungsverhaltnisse am Sudausgang des Roten Meeres. "Meteor" Forschung-Ergebnisse, Reihe A 4, 1–67.
Spall, M., Price, J., 1998. Mesoscale variability in Denmark Strait: the PV outflow hypothesis. Journal of Physical Oceanography 28, 1598–1623.
Washburn, L., Kaese, R., 1987. Double diffusion and the distribution of the density ratio in the Mediterranean waterfront Southeast of the Azores. Journal of Physical Oceanography 17, 12–25.
Wyrtki, K., 1971. Oceanographic Atlas of the International Indian Ocean Expedition. National Science Foundation.
Zenk, W., Tokos, K.S., Boebel, O., 1992. New observations of meddy movement south of the Tejo Plateau. Geophysical Research Letters 19, 2389–2392.
Zenk, W., Pinck, A., Becker, S., Tillier, P., 2000. The Float Park: a new tool for a cost-effective collection of Lagrangian time series with dual release RAFOS floats. Journal of Atmospheric and Oceanic Technology 17, 1439–1443.